ENERGY CONSERVATION

ORNL/Sub/80-7800/3 & 06

Technical and Economic Feasibility of Horizontal, Multiple Shallow-Well, and Deep-Well Ground Coupling for Residential Heat Pump Applications

Final Report

Robert D. Fischer

George H. Stickford, Jr.

BATTELLE
Columbus Laboratories
505 King Avenue
Columbus, Ohio 43201

Work performed for

OAK RIDGE NATIONAL LABORATORY
operated by
UNION CARBIDE CORPORATION
for the

U.S. DEPARTMENT OF ENERGY

OFFICE OF BUILDINGS ENERGY
RESEARCH AND DEVELOPMENT

ORNL/Sub--80-7800/6

DE84 006244

TECHNICAL AND ECONOMIC FEASIBILITY OF HORIZONTAL, MULTIPLE SHALLOW-WELL, AND DEEP-WELL GROUND COUPLING FOR RESIDENTIAL HEAT PUMP APPLICATIONS

FINAL REPORT

Prepared by

R. D. Fischer and G. H. Stickford, Jr.

October 14, 1983

BATTELLE
Columbus Laboratories
505 King Avenue
Columbus, Ohio 43201

Date Published: January 1984

Prepared under Subcontract 7800-19X06

OAK RIDGE NATIONAL LABORATORY
Oak Ridge, Tennessee 37830

Operated by

UNION CARBIDE CORPORATION

for the

UNITED STATES DEPARTMENT OF ENERGY

Contract No. W-7405-eng-26

TABLE OF CONTENTS

	Page
ABSTRACT	v
INTRODUCTION	1
METHODOLOGY	2
City Selection	2
Weather Data and Building Loads	3
Cost	7
Soil Properties	12
Water-Source Heat Pump Performance	18
Air-Source Heat Pump Performance	25
Horizontal Ground-Coil Model	25
Deep-Well Ground-Coil Model	28
Multiple Shallow-Well Model	32
PERFORMANCE COMPARISONS	38
COST COMPARISONS	54
CONCLUSIONS AND RECOMMENDATIONS	59
FUTURE WORK	62
REFERENCES	64

LIST OF TABLES

TABLE 1.	MONTHLY HEAT GAIN/LOSS FACTORS	5
TABLE 2.	BASE TEMPERATURES	6
TABLE 3.	AMBIENT TEMPERATURE PARAMETERS	8
TABLE 4.	RESIDENTIAL ELECTRICAL POWER COSTS	10
TABLE 5.	ESTIMATED COSTS FOR GROUND COILS	11
TABLE 6.	VALUES FOR THREE CONSTANTS FOR CALCULATING FAR-FIELD AND SURFACE EARTH TEMPERATURES	13
TABLE 7.	INFORMATION ON WATER TABLE AND SOIL LAYERS	15
TABLE 8.	PROPERTIES FOR SURFACE LAYER	16

TABLE OF CONTENTS
(Continued)

		Page
TABLE 9.	AVERAGE QUARTZ CONTENT OF SEDIMENTARY ROCK LAYERS	17
TABLE 10.	PROPERTIES OF SEDIMENTARY ROCK LAYERS WITH WATER IN PORES	19
TABLE 11.	PROPERTIES USED IN THE SWEDISH IEA PROGRAM	20
TABLE 12.	SOIL-LAYER PROPERTIES ASSUMED FOR EACH CITY	21
TABLE 13.	COST COMPARISON WITH HORIZONTAL GROUND COIL	40
TABLE 14.	PERFORMANCE COMPARISON WITH DEEP-WELL GROUND COIL	41
TABLE 15.	PERFORMANCE COMPARISON WITH MULTIPLE SHALLOW-WELL GROUND COIL	42
TABLE 16.	INLET FLUID TEMPERATURES WITH HORIZONTAL GROUND COIL	48
TABLE 17.	INLET FLUID TEMPERATURES WITH DEEP-WELL GROUND COIL	49
TABLE 18.	INLET FLUID TEMPERATURES WITH MULTIPLE SHALLOW-WELL GROUND COIL	50
TABLE 19.	SEASONAL COEFFICIENT OF PERFORMANCE WITH HORIZONTAL GROUND COIL	51
TABLE 20.	SEASONAL COEFFICIENT OF PERFORMANCE WITH DEEP-WELL GROUND COIL	52
TABLE 21.	SEASONAL COEFFICIENT OF PERFORMANCE WITH MULTIPLE SHALLOW-WELL GROUND COIL	53
TABLE 22.	PERFORMANCE COMPARISON WITH HORIZONTAL COIL	55
TABLE 23.	COST COMPARISON WITH DEEP-WELL GROUND COIL	56
TABLE 24.	COST COMPARISON WITH MULTIPLE SHALLOW-WELL GROUND COIL	57

TABLE OF CONTENTS
(Continued)

Page

LIST OF FIGURES

FIGURE 1. COEFFICIENT OF PERFORMANCE OF WATER-SOURCE HEAT PUMP 23

FIGURE 2. NODAL GEOMETRY FOR THE GROCS HORIZONTAL GROUND-COIL MODEL 27

FIGURE 3. NODAL GEOMETRY FOR DEEP-WELL GROUND COIL MODEL 29

FIGURE 4. COMPARISON OF BATTELLE DEEP-WELL MODEL WITH LINE-SOURCE THEORY 31

FIGURE 5. NODAL GEOMETRY FOR MULTIPLE SHALLOW-WELL MODEL WITH FOUR WELLS 34

FIGURE 6. NODAL GEOMETRY FOR MULTIPLE, SHALLOW-WELL MODEL WITH NINE WELLS 35

FIGURE 7. NODAL GEOMETRY FOR OUTER "STORE" OF MULTIPLE, SHALLOW-WELL MODEL 36

FIGURE 8. COMPARISON OF PREDICTED WELL TEMPERATURES WITH LINE-SOURCE THEORY 37

FIGURE 9. INLET FLUID TEMPERATURES TO HEAT PUMP WITH HORIZONTAL COIL IN PORTLAND, MAINE 43

FIGURE 10. INLET FLUID TEMPERATURES TO HEAT PUMP WITH HORIZONTAL COIL IN ATLANTA, GEORGIA 43

FIGURE 11. INLET FLUID TEMPERATURES TO HEAT PUMP WITH HORIZONTAL COIL IN WASHINGTON, D.C. 44

FIGURE 12. INLET FLUID TEMPERATURES TO HEAT PUMP WITH DEEP-WELL COIL IN PORTLAND, MAINE 46

FIGURE 13. INLET FLUID TEMPERATURES TO HEAT PUMP WITH DEEP-WELL COIL IN ATLANTA, GEORGIA 46

FIGURE 14. INLET FLUID TEMPERATURES TO HEAT PUMP WITH DEEP-WELL COIL IN WASHINGTON, D.C. 47

Preface

This report is one of a series of three (3) reports describing work undertaken for ORNL to assess the potential of ground-coil heat pump technology. The assessment focused on ground-coil heat exchanger design methods and related models and evaluated the performance and economics of three major design configurations for ground-coupled systems. Specific report titles include:

- "State-of-the-Art Survey of Existing Knowledge for the Design of Ground-Source Heat Pumps"
- "Models for Simultaneous Heat and Moisture Transfer in Soils"
- "Technical and Economic Feasibility of Horizontal, Multiple Shallow-Well, and Deep-Well Ground Coupling for Residential Heat Pump Applications"

ABSTRACT

An analytical assessment of ground-coupled heat pump systems in ten representative cities of the United States has shown that simple payback relative to air-source heat pumps is shortest for deep-well ground-coil systems and ranged from 8 to 10 years in three cities, 12 to 15 years in two cities, and above 30 years in Seattle which has low electrical rates and space conditioning loads. Simple payback with any of three types of ground-coil systems is non-existent in Phoenix and Houston, which have highest cooling loads and low water table. Simple payback with horizontal ground-coil systems was only slightly longer than with deep-well systems. Deep-well ground-coil systems had shorter simple payback than multiple shallow-well systems, particularly in areas where deep wells can be drilled into rock layers. Life-cycle costs with a real discount rate of 2.0 percent for horizontal and deep-well ground-coil systems were shorter than that for air-source systems in all cities except for Phoenix, Houston, and Seattle.

Seasonal heating coefficient of performance for the ground-coupled systems varied between 2.0 to 3.1 compared to 1.7 to 2.0 for air-source systems. Values of seasonal cooling coefficient of performance for ground-coupled systems were highest with the single deep-well coil. Cooling COP values with a horizontal coil were generally equal to or lower than values for air-source systems. Cooling COP values for air-source systems were higher than values for ground-coupled systems in southern climates with higher cooling loads.

FINAL REPORT

on

TECHNICAL AND ECONOMIC FEASIBILITY OF HORIZONTAL, MULTIPLE SHALLOW-WELL, AND DEEP-WELL GROUND COUPLING

to

UNION CARBIDE CORPORATION

from

BATTELLE
Columbus Laboratories

by

Robert D. Fischer
and
George H. Stickford, Jr.

October 14, 1983

INTRODUCTION

This report presents results from an analytical comparison of the performance and economics of residential space conditioning with three types of ground-coupled systems and air-source systems in ten metropolitan areas of the United States. The objective of this work was to establish a basis for direction of future work in ground coupling by developing performance and economic data for feasibility assessment of competitive systems.

This work has been a challenging, pioneering effort and was conducted with major inputs from ORNL in selecting the ten representative cities, characterizing the water table and soil layers in each city, and computing representative residential space conditioning loads and air-source heat-pump performance in each city.

Computer models were prepared for deep-well and multiple, shallow-well ground coupling which operate stably with time steps of about one-quarter hour. Execution times for annual runs were reduced to

reasonable levels by eliminating matrix inversion, used initially, with an explicit, forward, finite-difference approach in solution of the governing heat transfer equations. The model for the horizontal coil is based on the Brookhaven GROCS model with revisions to include thermal resistances due to convection within the tube and conduction through the wall of the plastic tubing.

Effects of the water table and different thermal properties of soil layers are explicitly accounted for in the well-type models. Moisture migration and freezing are not modeled, but different thermal properties for the soil above the water table are provided for winter and summer operation. All three computer models have similar subprograms for computing weather data and space conditioning loads, performance of the water-source heat pump, soil properties, convective heat-transfer coefficient at tubing walls with one of four brines, and far-field ground temperatures. The models are well suited for parametric study. For this initial effort, reasonable values for many variables had to be selected based on intuition and experience; however, the report does provide parametric data for major variables such as depth or length of the ground coil.

METHODOLOGY

A discussion of research methodology used in this feasibility study is presented in this section. Information is provided on city selection, weather data and building loads, cost, soil properties, water-source heat-pump performance, air-source heat-pump performance, and models for horizontal, deep-well, and multiple shallow-well ground coils.

City Selection

The representative cities for technical and performance evaluation of ground coils were selected by ORNL staff based on a review of climatic, geologic, and demographic features. These cities are:

1. Atlanta, GA
2. Pittsburgh, PA
3. Louisville, KY
4. Phoenix, AZ
5. Kansas City, MO
6. Houston, TX
7. Portland, ME
8. Seattle, WA
9. Washington, D.C.
10. Minneapolis, MN

Weather Data and Building Loads

Bin weather data and corresponding building loads for each of the ten cities were supplied by ORNL from runs with their seasonal energy use model, which was developed for climatic evaluation of the annual cycle energy system. These data consisted of the number of hours of occurrence of ambient temperature in 5F bins and corresponding loads for an 1800 sq ft building for each month of the heating and cooling seasons based on the long term average weather. The building insulation was appropriately selected for each city, and loads reflected occupancy, lighting, and solar influences.

These ambient temperatures and building loads can be used to accurately define the seasonal performance of air-to-air heat-pump systems but cannot be directly used in performance evaluation of ground-coil heat-pump systems. With ground-coil systems, performance is strongly influenced by the large thermal capacitance of the ground. Thus, an adequate simulation of ground-coil performance must include heat rejection or extraction on a continuous time basis so that the real effect of the earth thermal capacitance will be realized in long-term performance.

In our opinion, the building loads provided by ORNL provided a suitably-tailored adequate basis for comparative performance analysis in each city; however, these loads had to be apportioned on a continuous time basis. For this purpose, a simple UA heat loss or gain model with infiltration was used. The infiltration equation was based on that used in the

ORNL MAD program[1] which includes the effect of indoor-to-outdoor temperature difference and monthly value for wind velocity. A wind velocity of 9.7 mph was used for all cities except for Phoenix in which a value of 5.5 mph was used.

A two-step procedure was used to find seasonal heating and cooling UA factors and monthly base temperatures. Heat loss/gain factors were computed for each entry in the bin data, results were averaged for each month, and the monthly average was then used to recalculate the loads. Monthly values for the base temperature were obtained by a pattern-search procedure[2] to minimize the sum of the squares of differences between calculated and ORNL monthly loads. Calculated loads were weighted by the hours of occurrence at each bin temperature. The final form of the load equation is shown in Equations (1) to (5).

$$DT = (T_{base} - T_{amb})\ HEAT \quad (1)$$

$$Q_{ua} = UA\ DT \qquad (=0,\ \text{if } DT \text{ is} < 0) \quad (2)$$

$$DTS = (T_{set} - T_{amb})\ HEAT \quad (3)$$

$$ACHR = ACH\ (0.015 + 0.013\ VELW + 0.005\ DTS)/(0.659\ 60)$$

$$Q_{inf} = 1.086\ VOL\ ACHR\ DTS\ (=0,\ \text{if } DTS\ IS < 0) \quad (4)$$

$$Q_{ld} = (-1)\ HEAT\ (Q_{ua} + Q_{inf}) \quad (5)$$

where Q_{ua} = Heating/cooling load, Btu/hr

UA = Heat gain/loss factor, Btu/hr-F (see Table 1)

T_{base} = Base temperature, F (see Table 2)

T_{amb} = Ambient temperature, F

$HEAT$ = 1 for heating, = -1 for cooling

T_{set} = Set-point room temperature, F (heating: 68 F; cooling: 72 F)

VOL = House volume, ft^3 (14,400 ft^3)

ACH = No of air changes/hr (heating 0.5, cooling: 3.0)

$VELW$ = Wind velocity, mph (9.7 mph - all cities except Phoenix, which was 5.5 mph)

Table 1 shows the monthly UA heat gain/loss factors and Table 2 shows the base temperatures. Monthly totals of loads/gains calculated with Equation 5 agreed with ORNL values generally within less than 10 percent and most values agreed within less than 5 percent. As noted below, ambient temperatures were adjusted to obtain nearly exact agreement of these loads.

TABLE 1. MONTHLY HEAT GAIN/LOSS FACTORS*

CITY	SEASON	MONTH 1	2	3	4	5	6	7	8	9	10	11	12
(1) ATLANTA	HTG	338.	331.	329.	326.	-	-	-	-	-	280.	291.	313.
	CLG	-	-	-	770.	734.	709.	714.	690.	759.	912.	-	-
(2) PITTSBURGH	HTG	489.	466.	449.	398.	-	-	-	-	-	337.	407.	478.
	CLG	-	-	-	549.	666.	716.	748.	724.	726.	609.	-	-
(3) LOUISVILLE	HTG	467.	448.	436.	449.	-	-	-	-	-	391.	380.	432.
	CLG	-	-	-	707.	733.	688.	655.	652.	749.	832.	-	-
(4) PHOENIX	HTG	391.	421.	444.	399.	-	-	-	-	-	279.	358.	383.
	CLG	-	-	-	933.	693.	502.	465.	563.	580.	876.	-	-
(5) KANSAS CITY	HTG	504.	513.	517.	560.	-	-	-	-	-	472.	468.	508.
	CLG	-	-	-	539.	530.	523.	519.	509.	496.	577.	-	-
(6) HOUSTON	HTG	380.	389.	429.	458.	-	-	-	-	-	310.	351.	367.
	CLG	-	-	-	1015.	786.	698.	666.	687.	734.	948.	-	-
(7) PORTLAND,ME	HTG	576.	552.	510.	573.	-	-	-	-	-	585.	553.	563.
	CLG	-	-	-	700.	699.	689.	776.	799.	768.	717.	-	-
(8) SEATTLE	HTG	432.	389.	349.	346.	-	-	-	-	-	323.	364.	422.
	CLG	-	-	-	453.	441.	399.	439.	410.	388.	390.	-	-
(9) WASHINGTON,DC	HTG	392.	372.	348.	328.	-	-	-	-	-	287.	304.	368.
	CLG	-	-	-	546.	723.	635.	669.	673.	720.	822.	-	-
(10) MINNEAPOLIS, MN	HTG	521.	498.	469.	486.	-	-	-	-	-	427.	492.	520.
	CLG	-	-	-	628.	688.	651.	718.	750.	661.	666.	-	-

*In units of Btu/h-F.

TABLE 2. BASE TEMPERATURES

City	Base Temperature, F Heating	Cooling
(1) Atlanta	66.1	65.6
(2) Pittsburgh	65.0	65.3
(3) Louisville	60.4	64.7
(4) Phoenix	62.0	68.0
(5) Kansas City	58.2	63.7
(6) Houston	62.0	66.2
(7) Portland, ME	56.7	62.9
(8) Seattle	64.6	54.0
(9) Washington, D.C.	65.7	64.8
(10) Minneapolis, MN	60.5	65.5

The time duration of heating or cooling operation in each of the fringe months of April or October were apportioned based on the relative heating or cooling loads in the ORNL bin data. Any apparent cooling loads during the heating season are ignored and, similarly, any apparent heating loads during the cooling season are ignored.

With the load equation established, some means had to be provided for computing ambient temperature on a continuous time basis. Daily normals of ambient temperature were available from U.S. weather bureau data based on data from the years 1941 to 1970[3]. Monthly values of maximum ambient temperature and one-half of the difference between the maximum and minimum temperature were obtained from these data for each city. Ambient temperatures were assumed to vary similarly to the monthly average values.

Equation 6 shows the sinusoidal relationship used to compute ambient temperatures which are a maximum at 4 PM and a minimum at 4 AM.

$$T_{amb} = T_{ambm} + DT_{amb} \text{ Sin } (0.5 \text{ PI } (TC-4)/6-1)) \quad (6)$$

where T_{ambm} = Monthly maximum ambient temperature, F

DT_{amb} = One-half of the difference between maximum and minimum monthly ambient temperatures.

PI = 3.141596

TC = Time of day, hr.

Monthly totals of space conditioning loads were then computed with Equations 5 and 6 and compared to monthly values from the ORNL bin data. Values agreed fairly well except on the fringe months of April and October. The data were brought into nearly exact agreement by adjusting the monthly maximum ambient temperature using an automated search procedure. Table 3 shows the monthly maximum ambient temperature before (T) and after (T') adjustment and one-half of the difference between maximum and minimum temperatures (DT) for each city. The adjustment in maximum ambient temperature was quite low except for values in April and October.

Cost

Two types of economic analysis are provided, including simple payback and life-cycle costing. Simple payback is the number of years it

TABLE 3. AMBIENT TEMPERATURE PARAMETERS*

CITY	PARAMETER	MONTH 1	2	3	4	5	6	7	8	9	10	11	12
(1) ATLANTA	T,F	42.4	45.0	51.1	61.1	69.1	75.6	78.0	77.5	72.3	62.4	51.4	43.5
	T',F**	38.4	43.5	48.5	54.2	-	-	-	-	-	52.2	50.3	41.1
		-	-	-	72.8	71.0	75.1	76.7	77.2	72.8	68.8	-	-
	DT,F	9.0	9.5	10.0	10.3	9.9	9.0	8.5	8.9	8.9	10.1	10.5	9.2
(2) PITTSBURGH	T,F	30.6	32.0	40.4	52.5	62.2	71.3	74.6	73.0	66.5	55.8	44.1	33.3
	T',F	27.2	29.7	37.6	47.3	-	-	-	-	-	51.0	41.9	30.4
		-	-	-	73.0	65.3	69.6	71.6	71.2	67.0	70.3	-	-
	DT,F	6.8	7.5	8.5	10.0	10.1	9.7	9.4	9.6	10.2	10.3	7.5	6.5
(3) LOUISVILLE	T,F	33.3	35.8	44.0	55.9	64.8	73.3	76.9	75.9	69.1	58.1	45.0	35.6
	T',F	33.0	37.8	42.6	49.4	-	-	-	-	-	51.8	43.8	36.4
		-	-	-	72.4	68.9	74.4	77.6	76.8	71.8	72.5	-	-
	DT,F	8.7	9.2	10.0	11.0	10.8	10.4	10.4	10.9	11.4	12.2	9.9	8.5
(4) PHOENIX	T,F	51.2	55.1	59.7	67.7	76.3	84.6	91.2	89.1	83.8	72.2	59.8	52.5
	T',F	51.7	55.7	61.1	57.4	-	-	-	-	-	62.7	59.8	52.7
		-	-	-	73.0	77.8	84.4	88.1	87.7	83.8	74.7	-	-
	DT,F	13.6	14.2	14.8	15.9	16.6	16.9	13.6	13.1	14.6	15.4	14.9	13.9
(5) KANSAS CITY	T,F	27.1	32.3	40.7	54.2	64.1	73.0	77.5	76.5	68.0	57.6	42.3	31.3
	T',F	28.6	34.5	40.7	49.1	-	-	-	-	-	50.8	43.5	34.4
		-	-	-	71.9	69.4	76.2	80.3	80.2	73.4	69.1	-	-
	DT,F	8.6	9.1	10.0	10.5	10.1	9.8	10.5	10.7	10.8	10.6	9.1	8.0
(6) HOUSTON	T,F	53.9	56.7	62.2	70.2	76.4	81.9	84.3	84.3	79.9	72.2	62.5	56.5
	T',F	50.6	53.6	58.9	59.8	-	-	-	-	-	55.5	58.3	53.2
		-	-	-	72.7	76.3	81.1	83.2	82.8	79.2	73.3	-	-
	DT,F	8.0	8.1	8.4	7.8	7.9	7.9	8.0	8.2	8.2	9.1	8.6	8.2
(7) PORTLAND,ME	T,F	21.5	22.9	31.8	42.7	52.7	62.2	68.0	66.4	58.7	49.1	38.6	25.7
	T',F	22.6	24.8	30.7	41.5	-	-	-	-	-	47.4	38.9	26.7
		-	-	-	63.9	58.5	64.1	67.3	66.5	61.7	69.5	-	-
	DT,F	9.7	10.4	9.0	10.1	10.9	11.0	11.1	11.2	11.2	11.1	8.9	9.2
(8) SEATTLE	T,F	39.7	43.5	45.5	50.4	56.5	61.3	65.7	64.9	60.6	54.2	45.7	42.0
	T',F	38.9	42.7	42.5	47.6	-	-	-	-	-	50.9	42.8	40.0
		-	-	-	70.9	52.8	58.5	62.7	61.7	56.0	65.9	-	-
	DT,F	9.0	6.5	7.5	8.6	9.3	9.1	10.1	9.6	8.7	7.6	5.3	4.6
(9) WASHINGTON,DC	T,F	35.6	37.3	45.1	56.4	66.2	74.6	78.7	77.1	70.6	59.8	48.0	37.4
	T',F	32.2	34.4	41.2	49.8	-	-	-	-	-	51.3	46.7	35.0
		-	-	-	74.3	67.3	72.5	75.7	74.4	69.9	67.4	-	-
	DT,F	7.9	8.7	9.9	10.7	10.4	10.0	9.5	9.5	9.6	10.0	9.2	7.8
(10) MINNEAPOLIS,MN	T,F	12.2	16.5	28.3	45.1	57.1	66.9	71.9	70.2	60.0	50.0	32.4	18.6
	T',F	13.9	18.4	27.8	42.4	-	-	-	-	-	47.3	32.8	20.8
		-	-	-	74.9	64.1	70.4	72.9	72.0	65.8	71.0	-	-
	DT,F	9.0	9.0	8.65	10.4	10.8	10.2	10.5	10.6	10.7	10.8	8.2	8.0

* Parameters T' and DT are the same as T_{ambm} and DT_{amb} in Equation 6.

** Upper values are for heating and lower values are for cooling.

will take to recover the additional initial costs attributable to ground coupling in energy savings.

Present-value life cycle costs are based on the approach used in the ORNL MAD program[1] as shown in Equations (7) and (8).

$$PW = \frac{1 + r_e}{r_d - r_e} \left[1 - \left[\frac{1 + r_e}{1 + r_d} \right]^N \right] \tag{7}$$

$$LC = IC + PW\ (Po + MC) \tag{8}$$

where PW Present worth factor

r_e Annual price escalation rate of electrical power with zero inflation (0.0)

r_d Annual discount rate or cost of capital with zero inflation (0.02 and 0.10)

N Lifetime, yrs (20)

IC Initial installed cost of system attributable to use of ground coupling, $

Po Annual power cost with zero inflation (see Table 4)

MC Annual maintenance cost, $

It should be noted that use of Equation 8 assumes that maintenance costs and power costs are escalating at the same uniform annual rate. Maintenance costs were assumed to be similar for air- and water-source systems, so a value of 0.0 was used. Maintenance costs with air-source systems may be higher due to frosting problems; however, maintenance required by the brine circuit in water-source systems may offset costs attributable to frosting in air-source systems.

Table 4 shows values for electrical power costs in each city in January, 1982[4].

Costs assumed for coil material, boring or trenching, and placing the coil are listed in Table 5 for each of the three types of ground coils.

Coil material costs are based on use of medium density polyethylene material. Trenching and boring costs in unconsolidated soil for the horizontal coil and multiple shallow-well coil are based on estimates from Oklahoma State University[5]. The cost for boring in unconsolidated soil for a deep-well coil were escalated somewhat due to the use of a heavier duty, more costly drilling rig. Boring costs for mantle and bed rock are

TABLE 4. RESIDENTIAL ELECTRICAL POWER COSTS*

	City	$/KwH Heating	$/KwH Cooling
(1)	Atlanta	0.0489	0.0696
(2)	Pittsburgh	0.0591	0.0753
(3)	Louisville	0.0397	0.0544
(4)	Phoenix	0.0625	0.0747
(5)	Kansas City	0.0459	0.0681
(6)	Houston	0.0597	0.0751
(7)	Portland, ME	0.0667	0.0667
(8)	Seattle	0.0202	0.0163
(9)	Washington, D.C.	0.0470	0.0652
(10)	Minneapolis, MN	0.0480	0.0624

* Based on a monthly consumption of 2500 KwH from Reference 4.

TABLE 5. ESTIMATED COSTS FOR GROUND COILS

	Cost/ft, $
Horizontal Coil	
Coil Material	0.50
1-3/8" ID x .12" wall polyethylene tubing	
Trenching	0.75
Laying; backfilling ($25/hr at 100 ft/hr)	0.25
Deep-Well Coil	
Coil Material	
1-3/8" ID x .12" wall polyethlene supply tube	0.50
0.12" wall polyethylene casing; inside dia = 2.5"	0.88
5.0"	1.71
7.5"	2.55
Boring of 3.0 to 8.0" well, except as noted	
Unconsolidated soil	6.00
(3" well)	4.00
Mantle rock	7.00
Bed rock	8.00
Placing coil ($25/hr at 100 ft/hr plus allowance for casing joints)	0.40
Multiple, Shallow-Well Coil	
Coil Material	
1-3/8" ID x .12" wall polyethylene tubing, two tubes per bore)	1.00
Boring (Special purpose Ditch Witch unit limited to 110 ft deep)	
Unconsolidated soil	4.00
Mantle rock	6.00
Bed rock	8.00
Placing tubing ($25/hr at 100 ft/hr)	0.25

estimates. It was assumed that boring time in bed rock would be at least twice as long as in unconsolidated soil. Costs for coil placement are estimates based on use of a well developed approach for this activity.

Soil Properties

Far-field earth temperatures and surface temperatures were computed using the Kusuda relationship[6] for earth temperature at any depth as a function of time of year, thermal diffusivity of the earth, and three constants. Values for the three constants were not available for all cities, so these values were calculated from the long-term ambient temperature data for all cities. Calculated values agreed well with values published by Kusuda.

Equation (9) shows the Kusuda relationship for far-field earth temperatures. Values for the three constants are given in Table 6. Thermal diffusivity values were based on the values for the surface layer above the water table.

$$T_e = \bar{T}_e - DT_e \exp\left[-z \frac{PI}{ALF\ 8766}\right] \cos\left[\frac{2\ PI\ t}{8766} - z \frac{PI}{ALF\ 8766} - \theta\right] \quad (9)$$

where
- T_e = Earth temperature at depth, F
- $\bar{T}_e$ = Annual-average surface temperature, F
- DT_e = One-half amplitude of annual surface temperature
- t = Hour of year
- z = Depth, ft
- PI = 3.41596
- ALF = Thermal diffusivity of the surface layer, ft^2/hr
- θ = Phase angle, radians

It should be noted that far-field earth temperatures at depths below 40 to 50 ft are about equal to the annual-average surface temperature.

Characteristic values for density, specific heat, and thermal conductivity were selected as a function of depth based on appropriate values for representative layered soil and water table for each city.

TABLE 6. VALUES FOR THREE CONSTANTS FOR CALCULATING FAR-FIELD AND SURFACE EARTH TEMPERATURES

City	Annual Values at Surface		
	Avg. Temp,F	1/2 Amplitude, F	Phase Angle*, rad
(1) Atlanta	60.8	17.8	0.54
(2) Pittsburgh	53.0	22.0	0.55
(3) Louisville	55.6	21.8	0.57
(4) Phoenix	70.3	20.0	0.47
(5) Kansas City	54.0	22.0	0.56
(6) Houston	70.1	15.2	0.69
(7) Portland, ME	45.0	23.3	0.51
(8) Seattle	52.5	13.0	0.55
(9) Washington, D.C.	57.2	21.6	0.51
(10) Minneapolis, MN	44.1	29.9	0.55

* Phase angle = PI (2 TM/8766.-1)

where PI = 3.141596

TM = Time of year at which ambient temperature is maximum.

Note that long-term mean-monthly temperatures should be referenced to mid-month for use in a plot to determine time TM, because a shift of 1/2-month changes the phase angle significantly.

Table 7 summarizes information on water table and characteristics of soil layers supplied by ORNL staff. The water table varies from a high of 13 ft in Kansas City to a low of 150 ft in Phoenix.

Representative properties for the surface layer, summarized in Table 8, were provided by ORNL staff based on land-area-weighted samples. The somewhat surprising feature of these data are the similarity in values for the different cities. Values for Kansas City are approximated from other values and information in Table 7.

The wilting-dry values in Table 8 were used for cooling operation. Values for heating operation can be selected at some value between the wilting-dry and saturated values to account for moisture migration to cooler soil during heat extraction. These initial runs used saturated values.

Saturated values for the surface layer are used for any portion of the surface layer extending below the water table. A single value for layers below the water table is computed by weighting values for each layer according to the depth of layer.

Plots of thermal conductivity of many types of sedimentary rock were provided by ORNL staff. For most of these materials, thermal conductivity was plotted as a function of quartz content and porosity.

Table 9 shows average quartz content of various types of sedimentary rocks[7]. Porosity and density values were provided by ORNL from data compiled by U.S. Geological Survey from an analysis of many core samples at various depths. As expected, there was a wide variety in type of rock and variation in porosity in these data.

Thermal conductivity for weathered mantle rock was obtained from the plots using a porosity of 18 percent selected as a mean value representative of the core sample data. Thermal conductivity for bedrock was obtained at a value for porosity of 3 percent. Density values for mantle rock and bedrock were selected from the core sample data at samples with equivalent composition and porosity. Specific heat of solid rock is known to be in the range of 0.22 to 0.25 Btu/lbm-F. Density of solid rock is in the range of 160 to 170 lbm/ft^3. Specific heat and density for sedimentary rock with various levels of porosity can be computed by weighting the value for rock and water in pores by mass of each constituent.

TABLE 7. INFORMATION ON WATER TABLE AND SOIL LAYERS

	City									
	1 Atla.	2 Pitts.	3 Louis.	4 Phnx.	5 KC	6 Hous.	7 Port.	8 Sea.	9 WDC	10 MPL
Water Table, ft	40	25	65	150	13	100	20	50	28	45
Layer 1	0-40	0-25	0-65	0-150	0-13	0-100	0-20	0-50	0-28	0-45
(Surface)	See Table 8 for Characteristic Properties									
Layer 2	40-85 Mantle rock	25-60 Unconsolidated sediments of sandstone, shale, limestone, and coal	65-130 Glacial outwash and alluvium	150-2000 Conglomerate sand, silt, clay, gravel	13-20 Silty clay	100-2000 Unconsolidated sediments of sand, gravel, silt, and clay	20-40 Sand, gravel, till, peat	50-250 Unconsolidated sediments of sand, gravel, and till	28-46 Gravel broken sandstone	45-120 Saturated top soil
Layer 3	85- Bedrock (shale or sandstone porosity, ~3%	60- Bedrock (mostly shale or sandstone)	130- Bedrock (lime-stone, shale, and dolomite)	2000- Bedrock	20-106 Sand and gravel	2000- Bedrock	40-60 Mantle rock	250- Bedrock (shale, sandstone, coal, volcanic)	46-76 Mantle rock	120-170 Gravel, broken sandstone
Layer 4					106- Bedrock (layered limestone, shale, sandstone)		60- Bedrock (mostly slate, some granite)		76- Bedrock (shale or sandstone with low porosity)	170 Bedrock

TABLE 8. PROPERTIES FOR SURFACE LAYER

	City									
	1 Atla.	2 Pitts.	3 Louis.	4 Phnx.	5 KC	6 Hous.	7 Port.	8 Sea.	9 WDC	10 Minneapolis
Density, lbm/ft^3										
wilting dry	94.7	96.7	99.4	93.7	--	103.	99.0	96.3	103.	105.
saturated	116.	118.	119.	118.		120.	121.7	121.	124.	125.
saturated frozen	116.	118.	119.	118.		120.	121.7	121.	124.	125.
Specific Heat, Btu/lb-F										
wilting dry	0.260	0.244	0.257	0.226	--	0.271	0.215	0.205	0.220	0.225
saturated	0.397	0.384	0.381	0.387	--	0.376	0.367	0.368	0.353	0.349
saturated frozen	0.264	0.259	0.257	0.260	--	0.255	0.252	0.253	0.246	0.245
Thermal Conductivity, Btu/hr-ft-F										
wilting dry	0.509	0.510	0.536	0.526	--	0.541	0.512	0.552	0.757	0.605
saturated	0.760	0.781	0.780	0.814	--	0.779	0.987	1.021	1.109	0.958
saturated frozen	1.426	1.346	1.326	1.439	--	1.286	1.720	1.926	2.001	1.519

TABLE 9. AVERAGE QUARTZ CONTENT OF SEDIMENTARY ROCK LAYERS

Type of Rock	Quartz ($Si\ O_2$) Content, Percent
Sediment	58
Limestone	5
Sandstone	78
Shale	58
Ignaceous (Volcanic) Rock	59

Table 10 shows representative values for three types of sedimentary rock layers used in the analysis.

Table 11 shows values used in the Swedish work for the International Energy Agency for reference.

Table 12 shows soil-layer properties assumed for each city.

Water-Source Heat Pump Performance

From a performance evaluation of available water-source heat pumps conducted in September 1981[8], we decided to base performance characteristics for a water-source pump on the Carrier 50 WQ series. These units were available in four capacities from a nominal cooling capacity of 22,000 to 42,000 Btu/hr with 75 F inlet water temperature. Performance of the smallest unit in this series was known to be equal or better than that for competitive units, but brine-side pressure drop in the heat exchanger was judged to be excessive for ground coupling use. Units from other manufacturers were available which had good heating performance but could not be reversed for cooling operation. Other units had inherently low brine-side pressure drop and good heating performance but had much lower cooling performance.

Up-to-date performance information for the Carrier units was obtained from product literature. Well into our analysis, we found that Carrier downgraded performance of the new 50 VQ series to reduce costs. Results from preliminary runs with performance characteristics of the 50 VQ units showed less electrical power consumption with an air-source unit. It became apparent that selection of performance characteristics for the water-source heat pump is very important. We later found that heat rejection/extraction to the brine was too high in these preliminary runs and probably contributed to the poor performance of the ground-coil system.

In reassessing the needs for our program, we decided to base water-source heat-pump performance on data for the old Carrier WQ units with modifications to the heating coefficient of performance.

Figure 1 shows the heating coefficient of performance used in our study. Values for the TETCO unit (which cannot be reversed) and for the

TABLE 10. PROPERTIES OF SEDIMENTARY ROCK LAYERS WITH WATER IN PORES

Layer Description	Density, lbm/ft^3	Specific Heat, Btu/lbm-F	Thermal Conductivity, Btu/hr-ft-F
Gravel, Broken Sandstone	103	0.36	1.73
Mantle Rock	153	0.30	2.40
Bed Rock	164	0.26	3.30

TABLE 11. PROPERTIES USED IN THE SWEDISH IEA PROGRAM

Soil Type	Density, lbm/ft^3	Specific Heat Btu/lbm-F	Thermal Conductivity, Btu/hr-ft-F
Sand Partly Wet	118.6	0.191	1.04
Sand Saturated	124.9	0.334	1.73
Silt	137.3	0.287	0.809
Soft Clay	99.9	0.478	0.800
Hard Clay	137.3	0.289	1.04
Rock	156.0	0.215	1.73
Rock	156.0	0.334	1.73

TABLE 12. SOIL-LAYER PROPERTIES ASSUMED FOR EACH CITY

City	Layer Interval, ft.	Soil Description	Soil Moisture	Density, lbm/ft^3	Specific Heat, Btu/lbm-F	Thermal Conductivity Btu/hr-ft-F
1. Atlanta, GA	0-40	Top soil(1)	Dry(2)	94.7	0.26	0.51
			Wet	116.1	0.40	0.76
	40-85	Mantle rock	Wet	153.	0.30	2.4
	> 85	Bedrock	Wet	164.	0.26	3.3
2. Pittsburgh, PA	0-25	Top soil	Dry	96.7	0.24	0.51
	25-60	Top soil	Wet	118.	0.38	0.78
	> 60	Bedrock	Wet	164.	0.26	3.3
3. Louisville, KY	0-65	Top soil	Dry	99.4	0.26	0.54
	65-130	Top soil	Wet	119.	0.38	0.78
	> 130	Bedrock	Wet	164.	0.26	3.3
4. Phoenix, AZ	0-150	Top soil	Dry	93.7	0.23	0.53
	150-2000	Top soil	Wet	118.	0.39	0.82
5. Kansas City, MO	0-13	Top soil	Dry	100.	0.25	0.54
	13-20	Top soil	Wet	119.	0.38	0.78
	20-106	Sand/gravel	Wet	125.	0.40	1.4
	> 106	Bedrock	Wet	164.	0.26	3.3
6. Houston, TX	0-100	Top soil	Dry	103.	0.27	0.54
			Wet	120.	0.38	0.78
	> 100	Sand/gravel clay/mix	Wet	110.	0.45	1.3

(1) Top soil properties were compiled by ORNL

(2) Properties for winter operation were assumed to be wet values to account for the effect of moisture migration. "Wilting" dry values were used for summer operation.

TABLE 12. (Continued)

City	Layer Interval, ft.	Soil Description	Soil Moisture	Density, lbm/ft^3	Specific Heat, Btu/lbm-F	Thermal Conductivity Btu/hr-ft-F
7. Portland, ME	0-20	Top soil	Dry	99.0	0.22	0.51
	20-40	Top soil	Wet	122.	0.37	0.99
	40-60	Mantle rock	Wet	153.	0.30	2.4
	60	Bedrock	Wet	164.	0.26	3.3
8. Seattle, WA	0-50	Top soil	Dry	96.3	0.21	0.55
			Wet	121.	0.37	1.02
	50-250	Sand/gravel clay	Wet	110.	0.45	1.3
	250	Bed rock	Wet	164.	0.26	3.3
9. Washington, D.C.	0-28	Top soil	Dry	103.	0.22	0.76
			Wet	124.	0.35	1.11
	28-46	Gravel, broken sandstone	Wet	103.	0.36	1.73
	46-76	Mantle rock	Wet	153.	0.30	2.4
	76	Bed rock	Wet	164.	0.26	3.3
10. Minneapolis, MN	0-45	Top soil	Dry	105.	0.23	0.61
	45-120	Top soil	Wet	125.	0.35	0.96
	120-170.	Sand, gravel	Wet	125.	0.40	1.40
	170.	Bedrock	Wet	164.	0.26	3.3

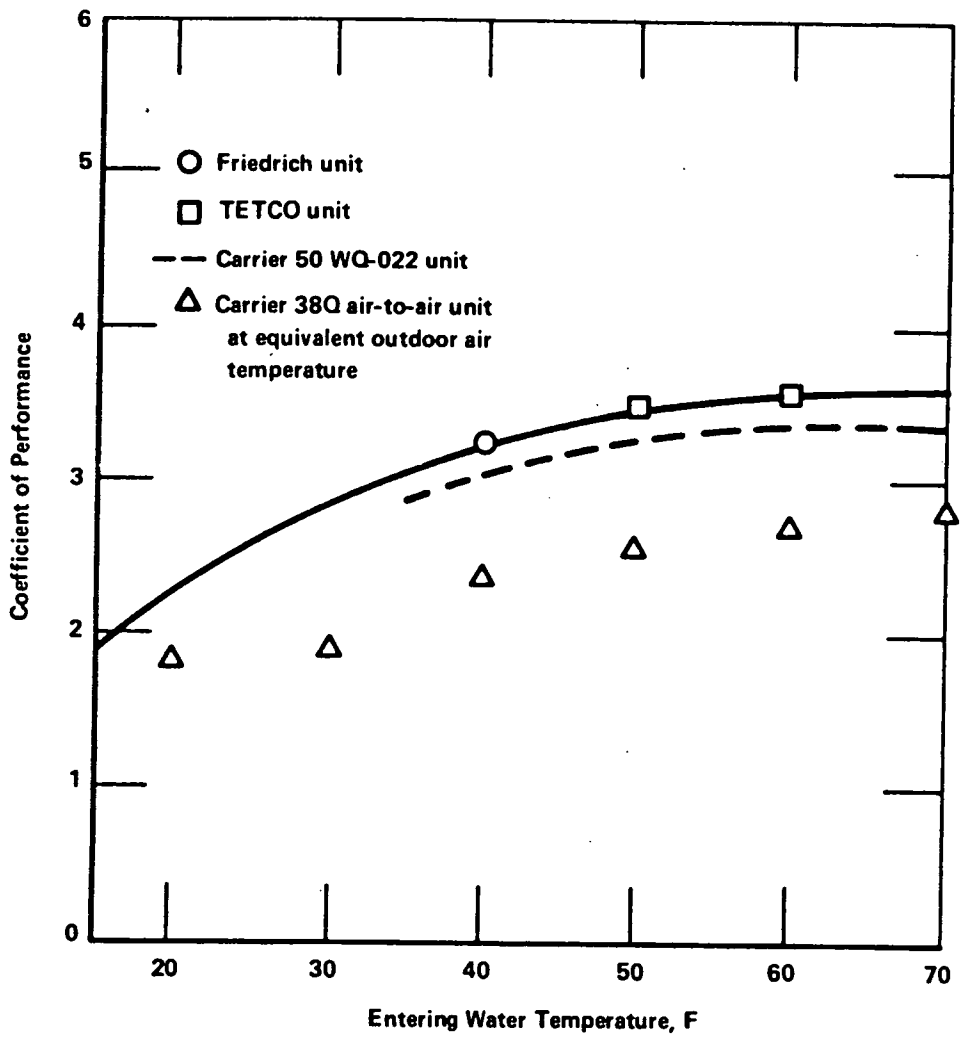

FIGURE 1. COEFFICIENT OF PERFORMANCE OF WATER-SOURCE HEAT PUMP

Friedrich unit fall on the selected curve. The shape of the curve is based on that for the smallest Carrier unit shown in Figure 1 as a dashed line. Heating coefficient of performance for the larger Carrier units become progressively lower with increasing size, probably due to an inadequately sized brine-to-refrigerant heat exchanger. By contrast, coefficient of performance for the series of air-to-air heat pumps used for comparison was about the same for all sizes, indicating that each size was optimized for good performance. Since all sizes of the baseline air-to-air units appear to be optimized, we feel justified in using a single curve for heating coefficient of performance for all sizes of water-source heat pumps.

Values for cooling and heating capacity and cooling coefficient of performance for all four Carrier 50 WQ units were fitted as linear functions of inlet water temperature for use in the program. With minor adjustment in capacity of one unit, these values appear to provide a realistic basis for a steady-state performance model in which effects of variations in inlet water temperature and mismatching will be reflected in system performance.

Electrical power consumption and heat extraction/rejection to the brine were then calculated from Equations (10) and (11).

$$KW = CAPY/(3413\ COP) + KWPUMP \tag{10}$$

$$Q_{rej} = (-1)\ HEAT\ (CAPY - HEAT\ (KW-KW_f)\ 3413E_c) + QPUMP \tag{11}$$

where

KW	Electrical power consumption, kW
CAPY	Space conditioning capacity, Btu/hr
COP	Coefficient of performance with penalty of blower motor
KW_f	Electrical power consumption of blower motor, kW (one value for each unit for both heating and cooling operation)
HEAT	= 1 for heating, = -1 for cooling
E_c	Correlation coefficient (separate values for each unit for both heating and cooling operation: ∿1.15 for heating, ∿1.19 for cooling).

KWPUMP Electrical power consumption of pump motor with 40 and 75 percent pump and motor efficiencies, respectively, kW.*

QPUMP Heat equivalent of pump work.

The heat pump was controlled to operate with 3 to 4 on-off cycles per hour, depending on stability requirements. The relative on-off time periods were apportioned to match the load. Performance degradation due to cycling operation is accounted for by multiplying electrical power consumption by a degradation factor (chosen to be 1.15) whenever the capacity of the unit exceeds the space-conditioning load. Heat extraction/rejection from or to an individual ground coil is apportioned to each coil based on the percentage of the total ground-contact coil area.

The selection of one of the four heat-pump units for any particular city is dependent on heating and cooling loads and brine temperatures during the coldest and warmest months. The initial sizes were selected based on results from matching heat pumps to the loads in each city during January and July and additional sizing data for air- and water-source heat pumps from ORNL.

Air-Source Heat Pump Performance

Performance and economics of the ground-coil space-conditioning system will be compared with that for an air-to-air heat-pump system. Performance data for representative air-to-air heat pumps were provided by ORNL from runs in which the size of heat pump for each city was selected based on lowest life-cycle cost. This series of heat pumps was designated "standard midline" in accord with characteristic performance of high quantity production units. Cycling losses were computed using C_D degradation factors of 0.25 for both heating and cooling. Defrosting losses were computed using Parken and Kelly frosting data[9].

Horizontal Ground-Coil Model

The model for horizontal serpentine ground coil is based on the GROCS model[10] developed by Brookhaven National Laboratory for use with

*Note: Pumping power typically averages 200-300 watts and accounts for only a small percentage (5-10%) of total electrical power consumption for these closed-loop ground-coupled heat pump systems.

TRNSYS[11]. To minimize computational time, the model uses a comparatively small number of large nodal volumes with "free" nodes in the vicinity of the coil bounded by "rigged" nodes. Temperature of each of the "rigged" nodes is computed by interpolation for each month as a function of depth for each timestep.

The GROCS program computes outlet brine temperature and soil temperature for each node in timesteps of 1 hour or less in response to time-dependent mass flow or inlet brine temperature. Thermal resistance for heat flows from the horizontal piping to the centroid of adjacent "free" nodes above and below the plane of the coil is computed using a steady-state conduction relationship which provides a means for evaluation of spacing between pipes.

In a previous design study[12] Battelle prepared a stand-alone version of this model, which can be run independently of TRNSYS, and made other changes to improve the utility of the program. A short driver program to replace TRNSYS provides execution and convergence logic and time-dependent heat extraction or rejection from the coil. At each timestep, the brine temperature to the field is computed by iteration from the known heat flow, fixed circulation rate, and computed brine temperature from the field. All inlet data arrays required in the original version are optionally computed from a few inputs. Effects such as piping length, burial depth or spacing can be evaluated by a change in value of that one parameter. Ground temperature tables in this modified version of GROCS are optionally computed using the Kusuda approach[6].

Concentric nodal geometry is used in this revised version as recommended by Andrews[10]. Figure 2 shows that the plane of the horizontal piping is represented by an equivalent circular plane. Note that the geometry of the nodal network is computed from a few inputs by using geometric similarity or ratios of values.

Further changes in the modified version of GROCS were made to couple the heat flow to the water-source heat pump. Additional terms were added to the calculation of average brine temperature to account for thermal resistance due to convective heat transfer at the wall of the coil and low thermal conductivity of the plastic coil material.

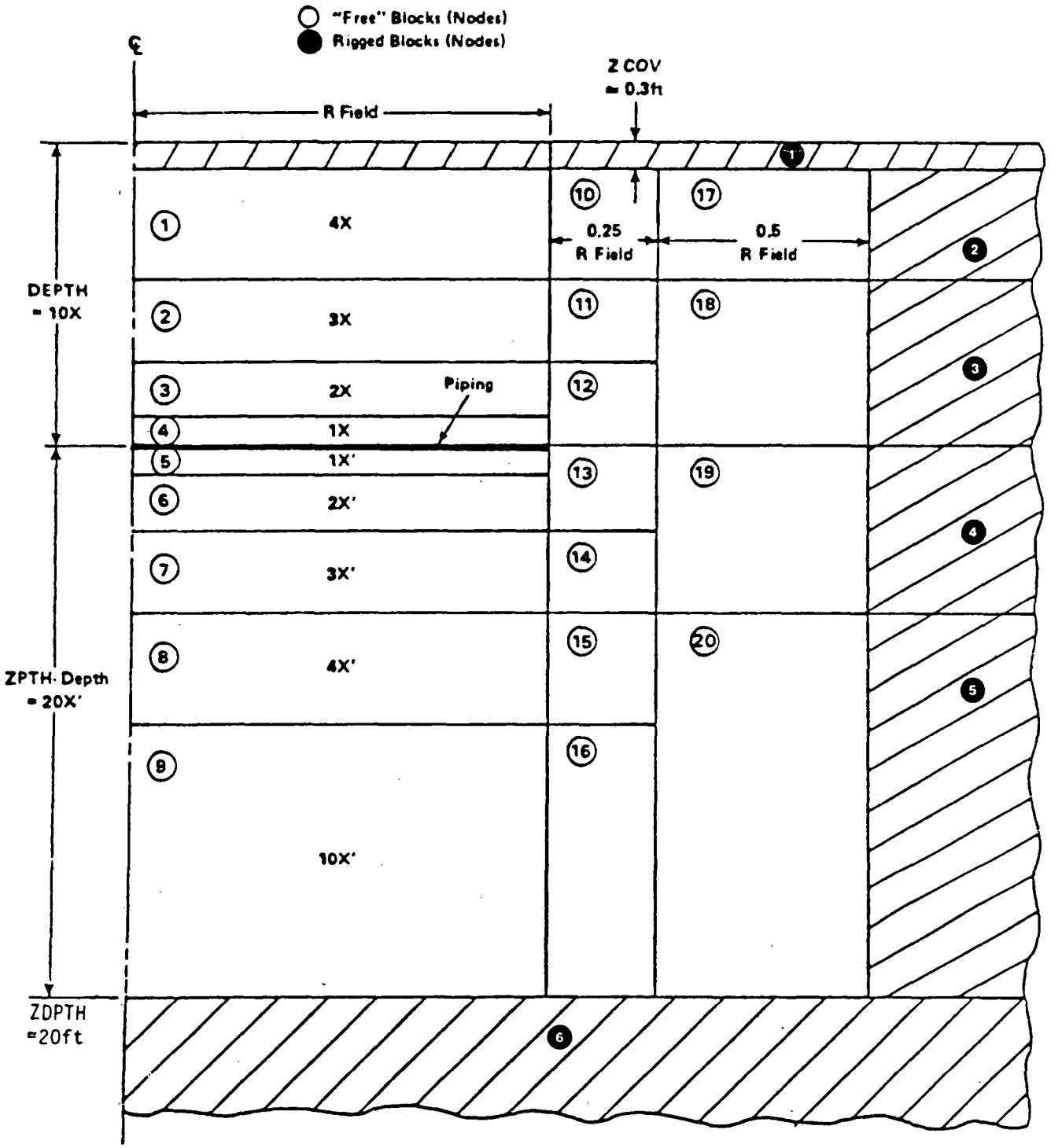

FIGURE 2. NODAL GEOMETRY FOR THE GROCS HORIZONTAL GROUND-COIL MODEL

Deep-Well Ground-Coil Model

A deep-well ground-coil model is being developed by ORNL staff but was not available for use at Battelle. Arrangements were made for Battelle to use the program on the ORNL computing system.

We elected to prepare our own deep-well model for the following reasons. We expected to make runs which spanned the entire heating and cooling seasons. Such operation would be prohibitively costly in computing time with the ORNL model, since this model uses a time step of about 10 seconds. Setting up for runs with all the peripheral items for working the same problem with different models, such as time-dependent ambient temperature, building loads, and heat extraction/rejection appeared to require more than a few days visit to the ORNL computing facility. Our initial attempts to set up linkage for remote batch operation at Battelle were blocked by our inability to communicate with the ORNL DEC-10 system on which the ORNL model is run.

Figure 3 shows the nodal geometry of the deep-well model prepared for this program. Thermal capacitances of the pipe and casing material are ignored so that the lowest thermal capacitance will be high enough to permit time steps of one-fourth hour or more without stability problems. This goal has been achieved.

As shown in Figure 3, the model is segmented into six nodes in the depth coordinate. The bottom layer extends from the water table to the bottom of the well and is segmented into three layers. The unsaturated upper layer is segmented into three nodes extending from the bottom of a thin surface layer down to the water table. Temperatures in the surface layer and on outer and lower boundaries are computed by the Kusuda relationship[6].

There are five brine nodes including an external node to represent the brine inventory in connecting piping and heat exchanger. All heat extraction/rejection energy flows are coupled to this node. Fluid nodes in the depth coordinate are segmented at the water table. There are six soil nodes in the radial coordinate with relative spacing about as shown in Figure 3. Note that the radial widths of the inner pipe wall and the casing are exaggerated in Figure 3 for illustrative purposes.

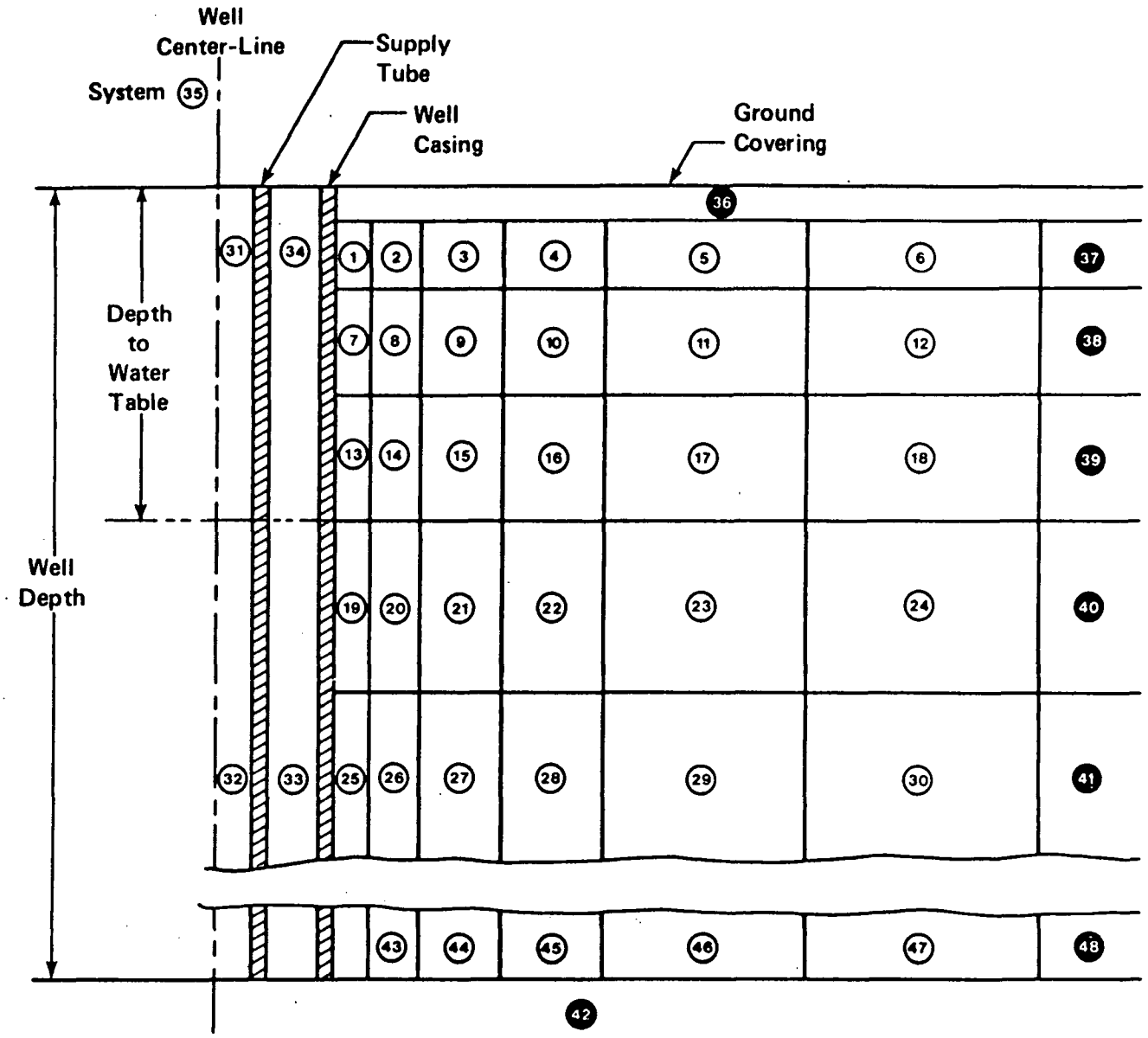

FIGURE 3. NODAL GEOMETRY FOR DEEP-WELL GROUND COIL MODEL

Thermal resistances due to convective heat transfer at the walls of the inner pipe and casing are accounted for. Convective heat-transfer coefficients are computed as a function of mean brine temperature at time intervals of about 3 days for one of the following brine fluids: ethylene-glycol, propylene-glycol, calcium chloride, and methanol, using a subprogram prepared previously[8] with revision to include the effect of entrance length on the laminar convective heat transfer coefficient for flow from the bottom to top of the annulus.[13]

A network analysis approach for transient heat transfer is used in this model. The same approach has been used by Battelle staff previously for analysis of transient heat transfer in passive solar walls[14] and solidification of molten copper. New node temperatures are computed for each timestep from mean values for that node and old values for surrounding nodes. This approach results in a matrix of first-order differential and algebraic equations which must be solved at each timestep by matrix inversion. The thermal conductance values for heat flow between coupled nodes are calculated from the nodal geometry and thermal properties of each node. These calculations were programmed so that variable properties for each node can be added later with relatively minor revision. Thermal properties are provided from data arrays for layers of unsaturated and saturated soil in each city. Properties for soil layers below the water table are merged into a single value by apportioning values by depth of layers. Nodal geometry is computed from a few input values.

Figure 4 shows source temperatures computed with the Battelle deep-well model and values computed with line-source theory[15] prepared for checking out the model and modeling strategy. Properties for all nodes were fixed at representative values and thermal conductances with inner-pipe nodes and the system node were decoupled for this run. Heat extraction from the two annuli nodes was apportioned according to the depth of each node.

Good agreement shown in Figure 4 was obtained only after the initial timestep was decreased to a few seconds. After four timesteps, the timestep is increased to one-fourth hour. No apparent instability was

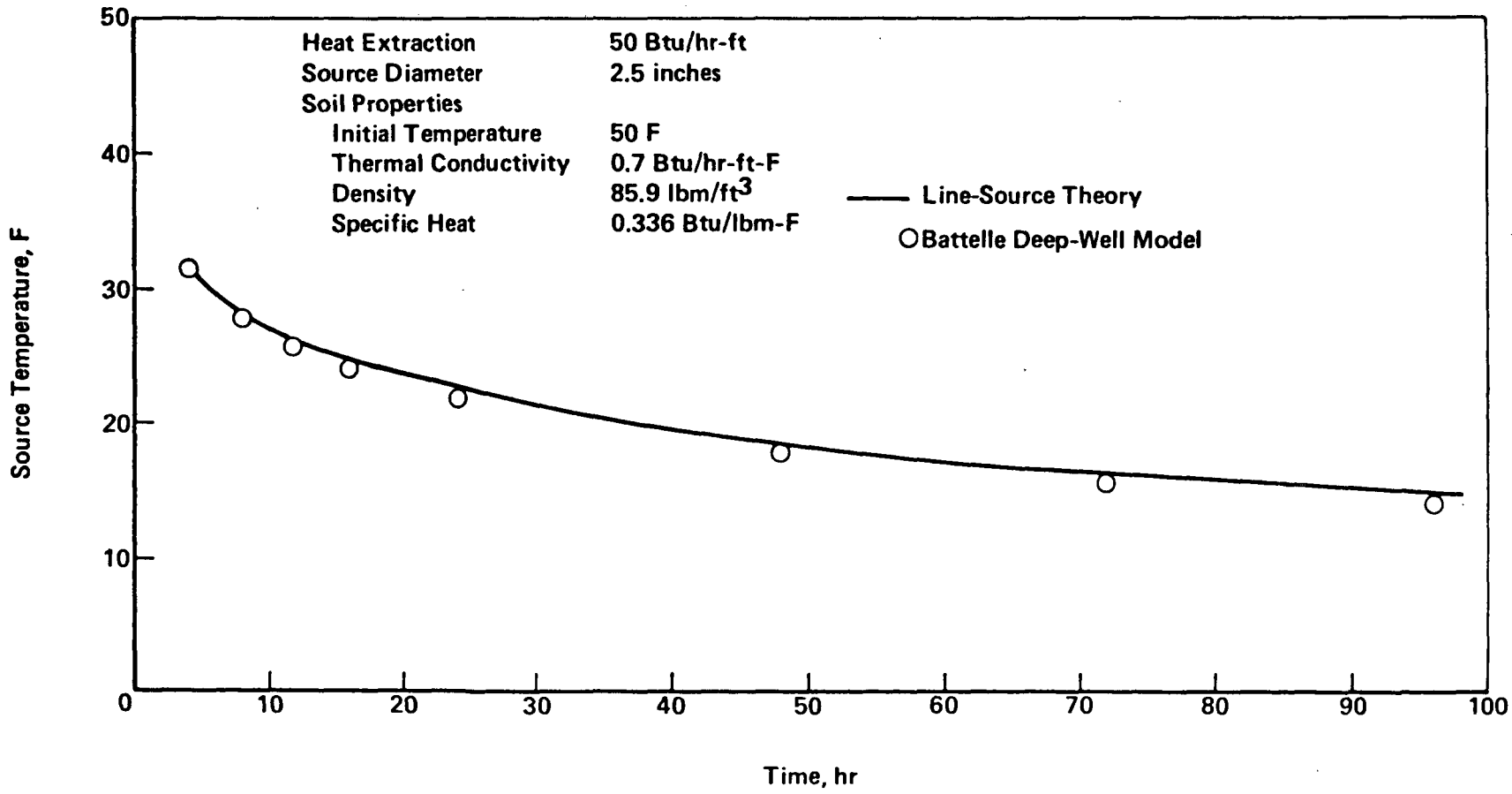

FIGURE 4. COMPARISON OF BATTELLE DEEP-WELL MODEL WITH LINE-SOURCE THEORY

observed in later runs with timesteps as high as one hour. Stability was further improved prior to these runs with the addition of the external system node.

While attempting to use this model for yearly runs, it became apparent that further development was needed to reduce computing time from initial values of approximately 780 seconds per month. We decided to use an explicit, forward, finite-difference approach in which new temperatures for each node are computed directly without matrix inversion. A stability criterion is utilized to fix minimum values for the timestep to preserve accuracy. This same approach has been used for constructing many large transient heat transfer models at Battelle. The GROCS program uses a similar approach[16], but the stability criteria is ignored because large blocks are used.

With the explicit method, computing time for one month was reduced to about 42 seconds, which is comparable to about 36 seconds for the horizontal model based on the GROCS program. The original nodal geometry of the model shown in Figure 3 has been preserved for use in short duration runs to evaluate the effect of material and wall thickness of the inner pipe. However, the large thermal coupling between fluid nodes caused instability with the explicit approach. When explicit solution is requested, the nodal geometry is revised by lumping the thermal capacitance of all fluid nodes into one node in contact with the casing wall. Thermal resistance due to convection at the casing wall is computed as in the more detailed model. Inlet fluid temperature to the heat pump is computed by adding or subtracting one-half of the absolute change in temperature of the brine at the heat exchanger, apportioned to each coil, to or from the fluid node temperature for heating and cooling operation, respectively.

Multiple Shallow-Well Model

A multiple shallow-well model is being used in Sweden in support of research on multiple shallow-well ground coils; however, the computer program for this model is proprietary and could not be used on our program. Descriptive information on the Swedish model provided by ORNL was helpful in formulating our approach to developing such a model.

Figures 5 and 6 show nodal geometry for configurations with four vertical coils in a square grid and with nine coils in a 3 x 3 square grid. The square grid was selected because this configuration will have the lowest peripheral heat loss and highest carryover of stored energy from season to season.

The inner "store" is modeled in the one-eighth segment because no heat flows across the inner boundaries of the segment due to symmetry of the four coils. Heat is exchanged at the outer boundary and at the top and bottom of the nodes. Two sets of nodes in the depth coordinate are provided for explicit modeling of the water table, as in the deep-well model. The fluid is modeled as a single node with an additional volume added to represent a portion of the system volume. The rationale for using a single fluid node is that with side-by-side supply and return lines, adjacent soil will experience a mean fluid temperature. The effective circumference of the fluid node in contact with the soil is computed by assuming this value is equal to 0.92 of the total circumference of the two side-by-side supply and return tubes assumed per coil. Thermal conductances and capacitances are computed from nodal geometry and properties for the earth above and below the water table.

Figure 7 shows the nodal geometry of the outer "store" surrounding the square grid of coils. The nodal geometry explicitly accounts for the water table. Temperatures in the surface layer and at boundary nodes are computed by the Kusuda relationship[6].

Figure 8 shows source temperatures computed with the Battelle multiple shallow-well model and values computed with line source theory[15] prepared for checking out the model and modeling strategy. This exercise helped to identify a number of errors in conductance equations and provided verification for the selection of the path length for heat exchange between the coil and the adjacent soil node. As with the deep-well model, the initial few timesteps had to be reduced to a few seconds to get the good agreement shown in Figure 8. After four small timesteps, the timestep can be increased to one-fourth hour with good stability.

To minimize computing times, new values for temperatures in the outer "store" are computed at every fourth timestep of the inner "store".

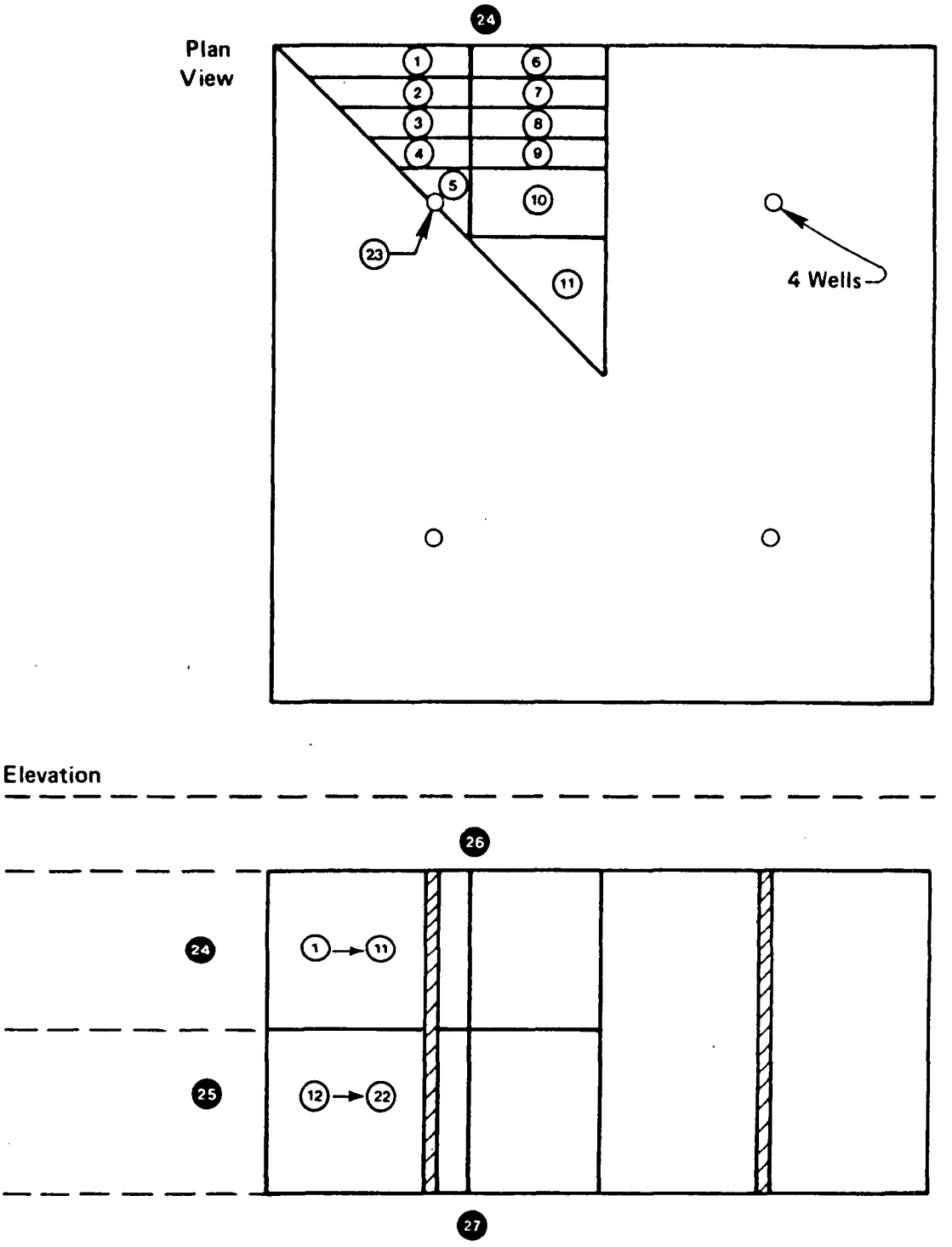

FIGURE 5. NODAL GEOMETRY FOR MULTIPLE SHALLOW-WELL MODEL WITH FOUR WELLS

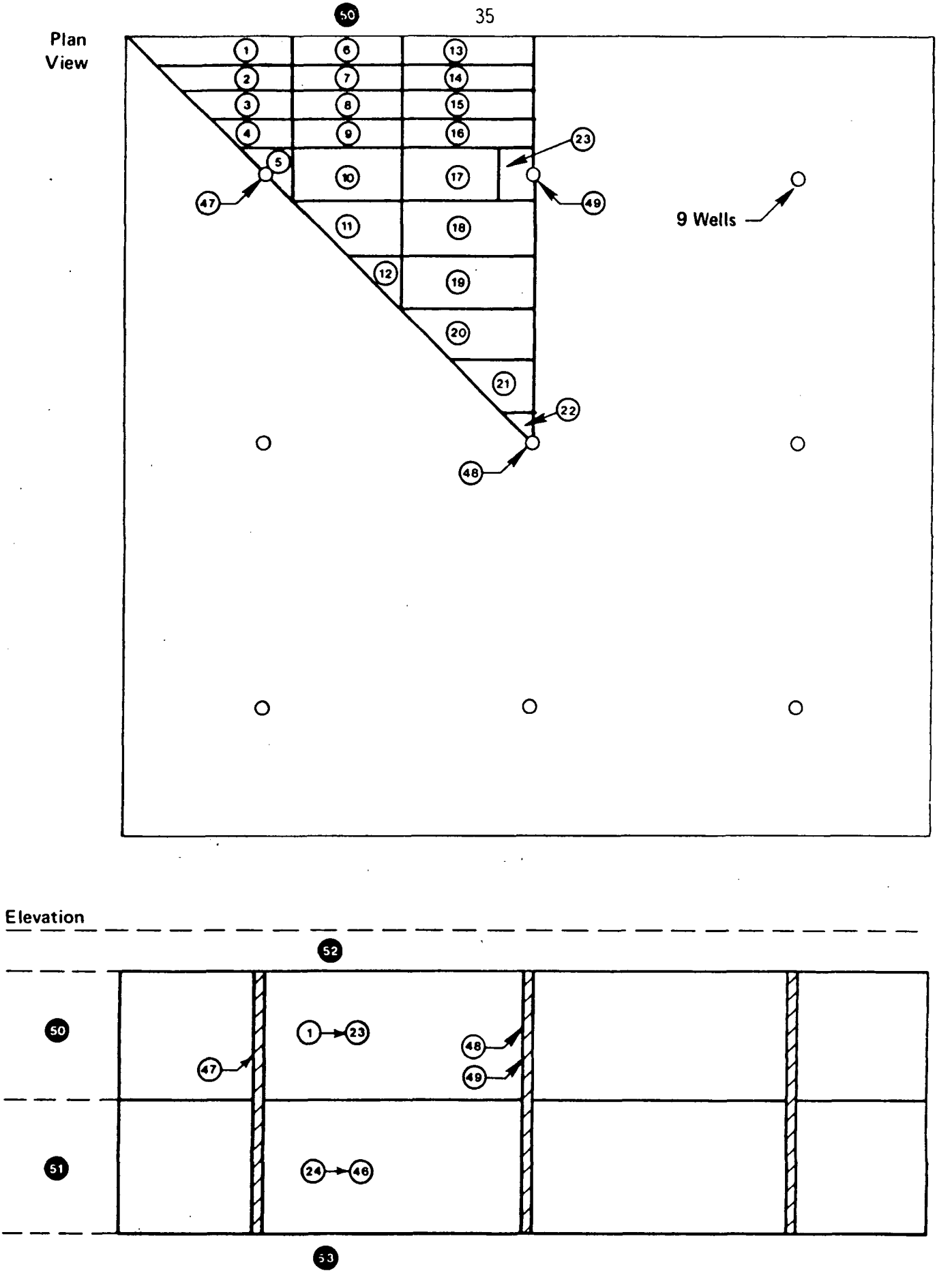

FIGURE 6. NODAL GEOMETRY FOR MULTIPLE, SHALLOW-WELL MODEL WITH NINE WELLS

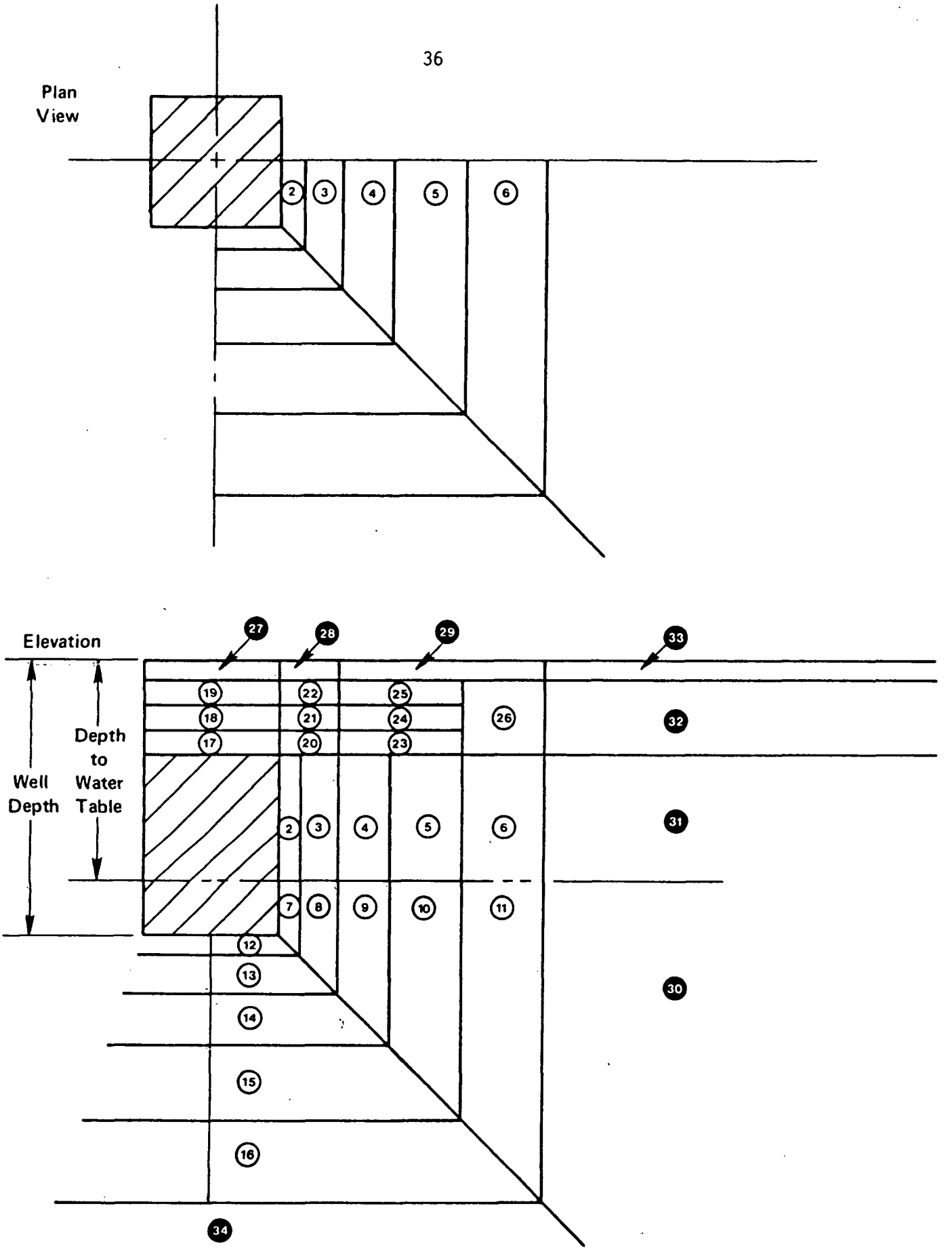

FIGURE 7. NODAL GEOMETRY FOR OUTER "STORE" OF MULTIPLE, SHALLOW-WELL MODEL

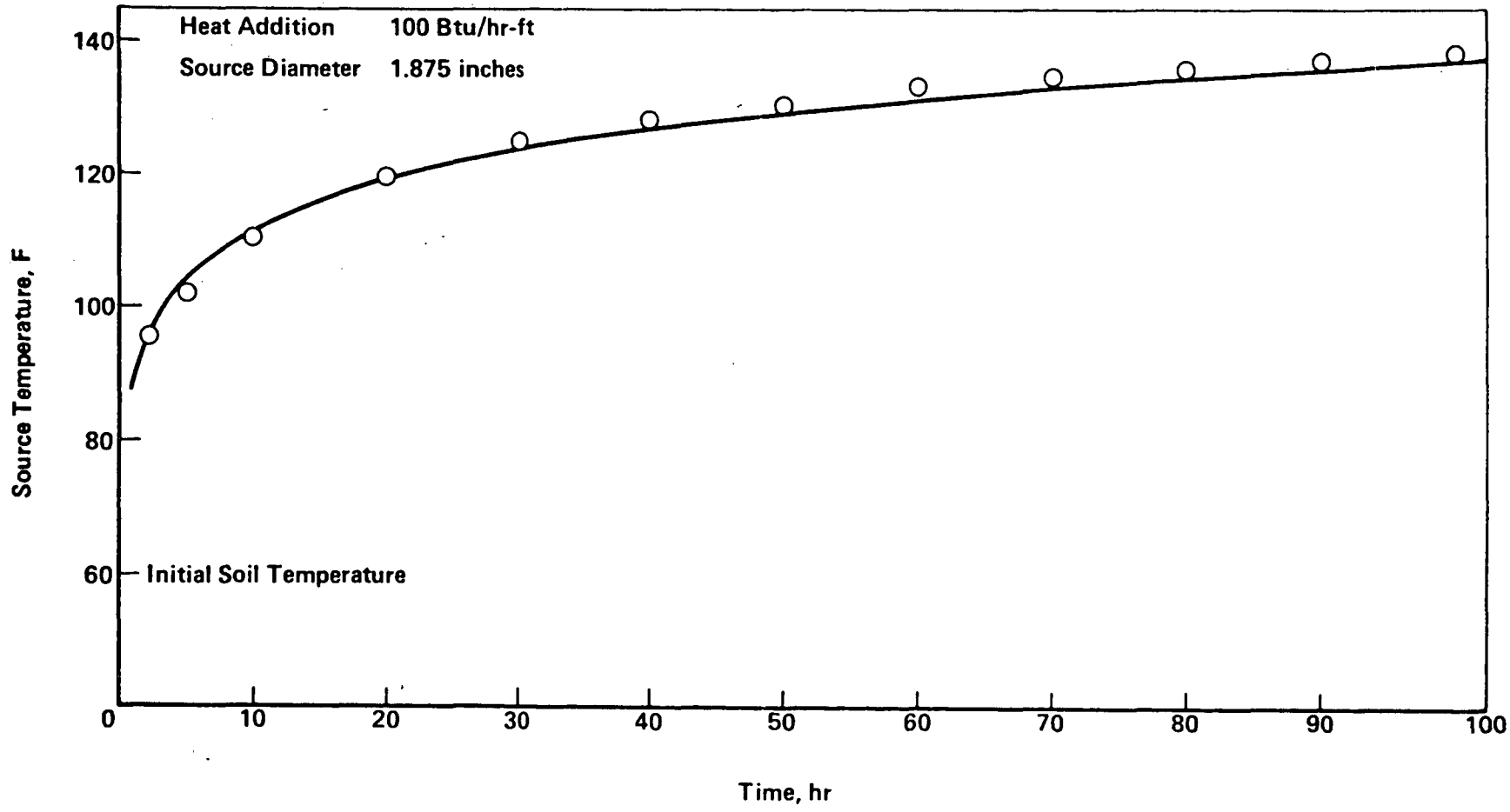

FIGURE 8. COMPARISON OF PREDICTED WELL TEMPERATURES WITH LINE SOURCE THEORY

Computing time with the original approach with matrix inversion was dramatically reduced from about 340 sec per month to about 50 sec for the 2 x 2 model and from about 2800 sec per month to 63 sec for the 3 x 3 model with an explicit, forward, finite difference approach as used in the deep-well model. No change was made in modeling of the fluid nodes with the explicit approach, since a single node was used for each coil from the outset.

Inlet fluid temperature to the heat pump is computed as in the deep-well model by adding or subtracting one-half of the absolute change in temperature of the brine at the heat exchanger, apportioned to each coil, to or from the fluid node temperature for heating or cooling, respectively.

PERFORMANCE COMPARISONS

A total of 59 yearly runs provide performance data on the three types of ground coil systems and air-source systems in the 10 cities. More data are available for the cities Portland, ME; Atlanta, GA; and Washington, D.C., since these cities were chosen for original analysis and limited parametric study. Additional runs were made for some of the ground coil systems in attempts to define optimum coil geometry or to improve cost predictions.

All three ground-coil models were set up with identical subprograms for auxiliary data such as weather and load data, water-source heat pump performance, soil properties, and costs. Methanol brine was used for all runs. The convective heat-transfer coefficient at the tubing or casing wall was updated about every three days at the hour for maximum heating or cooling. Runs were begun in each city at the start of the heating season in October and continued for 8,760 hours. To minimize computing time, no attempt was made to adjust initial earth temperatures to values influenced by ground-coil operation during the previous season. Rather, initial earth temperatures were set to values appropriate for the depth using the Kusada relationship[6]. Depth of the horizontal coil was 4.0 ft.

Appropriate heat flows and energy-consumption values were summed at each timestep to provide data for checking energy balances and assessing

seasonal energy consumption. Excess heat pump capacity was accounted for by reducing the on-time for the timestep by the ratio of building load to capacity. Insufficient heating capacity was assumed to be supplemented with electric resistance heating to fully meet the heating load. Any deficit in cooling capacity was summed for inspection, so that results would not be biased toward heat pumps with an inadequate cooling capacity.

Tables 13 to 15 show summed heating and cooling performance data for runs with horizontal, deep-well, and multiple, shallow-well ground coils compared to that for air-source systems. Values of electric power consumption for heating were lower with the ground-coil systems for all but one run. For cooling, electric power consumption was lower in 33 of the 59 runs. Of the 26 instances of higher cooling electric power consumption with ground-coil systems, some were due to inadequately sized ground coils, and the balance were in Phoenix and Houston where ground-coil performance was poor due to high cooling load and low water table.

Values for the ground-coil cooling deficit are provided because it was not possible to precisely match the capacity of the water-source heat pump to the load in every city with each ground-coil configuration. Large values of the parameter indicates that either the heat pump or ground coil is undersized for the cooling load.

On-time values can be used to assess how closely the heat pump is matched to heating or cooling loads. Lower values provide an indication that substantial cycling operation was experienced in comparison to that for the other type of heat pump.

Figures 9 to 11 show the effect of coil length on inlet fluid temperatures to the heat pump with a horizontal-coil system in Portland, ME, Atlanta, GA, and Washington, D.C. Below freezing brine temperatures would be experienced even with the longest coil in Portland, ME due to high heating load and low earth temperatures. Lowest temperatures would be somewhat higher than those shown on Figure 9 in an actual installation, because freezing of the soil about the tubing was not modeled. Both the latent heat of fusion and better thermal properties of frozen soil would help to maintain higher temperatures in the coldest months.

TABLE 13. PERFORMANCE COMPARISON WITH HORIZONTAL COIL

CITY	COIL LENGTH, FT	ELECTRIC POWER, KWH HEATING GROUND COIL	HEATING AIR SOURCE	COOLING GROUND COIL	COOLING AIR SOURCE	SUPPLEMENTAL RESISTANCE HEATING, KWH GROUND COIL	HEATING AIR SOURCE	GROUND COIL COOLING DEFICIT, PCT OF TOTAL	ON TIME, HR HEATING GROUND COIL	HEATING AIR SOURCE	COOLING GROUND COIL	COOLING AIR SOURCE
PORTLAND, ME	900	9664	11179	1734	1547	1417	1822	0.00	3288	2770	324	330
	1200	9415		1472		989		0.00	3147		304	
	1500	9291		1361		767		0.00	3050		294	
ATLANTA, GA	700	3479	4946	5883	3940	0	279	0.00	1667	1695	1496	1283
	900	3394		4490		0		0.00	1557		1360	
	1100	3351		3920		0		0.00	1491		1295	
WASHINGTON DC	700	5468	7220	3878	3061	0	530	0.00	1892	2276	851	899
	1000	5210		3038		0		0.00	1767		786	
	1300	5108		2760		0		0.00	1701		757	
PITTSBURGH, PA	1200	7866	9853	1898	2117	30	1489	0.00	2718	2745	518	523
LOUISVILLE, KY	900	5119	6762	5090	3964	0	574	0.00	1762	2142	1107	1156
	1100	4977		4253		0		0.00	1693		1047	
PHOENIX AZ	1600	1383	2085	10456	7439	0	0	0.00	364	489	1593	1596
	1800	1386		9587		0		0.00	359		1548	
KANSAS CITY, KY	1000	5949	7345	4544	4016	0	1216	0.00	2046	2366	1062	1161
	1100	5858		4218		0		0.00	2006		1037	
HOUSTON TX	1300	1268	1960	9450	6833	0	5	0.00	373	543	1941	1797
	1500	1268		8338		0		0.00	367		1872	
SEATTLE, WA	500	5750	7010	1862	1102	0	190	0.00	2016	2615	348	415
	700	5317		1258		0		0.00	1853		306	
MINNEAPOLIS MN	900	10770	12799	2290	2230	4114	3469	0.00	3712	2836	441	387
	1200	10619		1972		3315		0.00	3632		416	

TABLE 14. PERFORMANCE COMPARISON WITH DEEP-WELL GROUND COIL

CITY	COIL DEPTH, FT	ELECTRIC POWER, KWH HEATING GROUND COIL	HEATING AIR SOURCE	COOLING GROUND COIL	COOLING AIR SOURCE	SUPPLEMENTAL RESISTANCE HEATING, KWH GROUND COIL	HEATING AIR SOURCE	GROUND COIL COOLING DEFICIT, PCT OF TOTAL	ON TIME, HR HEATING GROUND COIL	HEATING AIR SOURCE	COOLING GROUND COIL	COOLING AIR SOURCE
PORTLAND, ME	200	8786	11178	1032	1547	975	1822	0.00	3080	2770	264	330
	280	8436		998		428		0.00	2883		260	
	360	8306		982		204		0.00	2766		257	
ATLANTA, GA	120	3439	4946	4627	3940	0	279	0.00	1645	1695	1370	1283
	180	3261		3285		0		0.00	1404		1209	
	240	3217		2978		0		0.00	1323		1158	
WASHINGTON DC	140	5199	7220	2636	3061	0	530	0.00	1804	2276	749	899
	200(1)	5047		2531		0		0.00	1722		736	
	200	4891		2335		0		0.00	1639		713	
	200(2)	4829		2242		0		0.00	1598		701	
	260	4789		2214		0		0.00	1566		697	
PITTSBURGH, PA	240	7334	9853	1408	2117	0	1489	0.00	2545	2745	460	523
	280	7172		1383		0		0.00	2456		457	
LOUISVILLE, KY	210	4795	6762	3448	3964	0	574	0.00	1651	2142	976	1156
	250	4635		3149		0		0.00	1583		942	
PHOENIX AZ	400	1324	2085	10520	7439	0	0	0.00	331	489	1632	1596
	500	1335		8583		0		0.00	326		1508	
KANSAS CITY, KY	210	5477	7345	3066	4016	0	1216	0.00	1896	2366	926	1161
	250	5318		2898		0		0.00	1813		904	
HOUSTON TX	340	1239	1960	8323	6833	0	5	0.00	343	543	1878	1797
	400	1240		7240		0		0.00	340		1799	
SEATTLE, WA	200	5287	7010	786	1102	0	190	0.00	1860	2615	255	415
MINNEAPOLIS MN	170	11450	12799	1748	2230	6188	3469	0.00	3971	2836	399	387
	250	10076		1478		3164		0.00	3637		371	

(1) Inside diameter of casing changed from 5.0" to 2.5"
(2) Inside diameter of casing changed from 5.0" to 7.5"

TABLE 15. PERFORMANCE COMPARISON WITH MULTIPLE SHALLOW-WELL GROUND COIL

CITY	COIL NO OF WELLS	COIL DEPTH, FT	ELECTRIC POWER, KWH HEATING GROUND COIL	ELECTRIC POWER, KWH HEATING AIR SOURCE	ELECTRIC POWER, KWH COOLING GROUND COIL	ELECTRIC POWER, KWH COOLING AIR SOURCE	SUPPLEMENTAL RESISTANCE HEATING, KWH GROUND COIL	SUPPLEMENTAL RESISTANCE HEATING, KWH AIR SOURCE	GROUND COIL COOLING DEFICIT, PCT OF TOTAL	ON TIME, HR HEATING GROUND COIL	ON TIME, HR HEATING AIR SOURCE	ON TIME, HR COOLING GROUND COIL	ON TIME, HR COOLING AIR SOURCE
PORTLAND, ME	9	80	9042	11178	1015	1547	457	1822	0.00	2970	2770	258	330
ATLANTA, GA	9	40	3569	4946	6134	3940	0	279	1.20	1769	1695	1717	1283
	9	50	3382		4164		0		0.00	1591		1322	
	9	60	3320		3485		0		0.00	1459		1236	
WASHINGTON DC	9	46	5277	7220	2723	3061	0	530	0.00	1812	2276	755	899
	9	60	5025		2419		0		0.00	1676		720	
PITTSBURGH, PA	9	70	7837	9853	1424	2117	26	1489	0.00	2720	2745	459	523
LOUISVILLE, KY	4	110	4957	6762	4108	3964	0	574	0.00	1708	2142	1036	1156
PHOENIX AZ	4	100	1371	2085	10918	7439	0	0	0.00	337	489	1660	1596
KANSAS CITY, KY	4	100	5534	7345	3203	4016	0	1216	0.00	1899	2366	940	1161
HOUSTON TX	9	80	1260	1960	11091	6833	0	5	.06	356	543	2196	1797
	9	100	1265		10365		0		0.00	352		2022	
SEATTLE, WA	4	70	5330	7010	859	1102	0	190	0.00	1865	2615	265	415

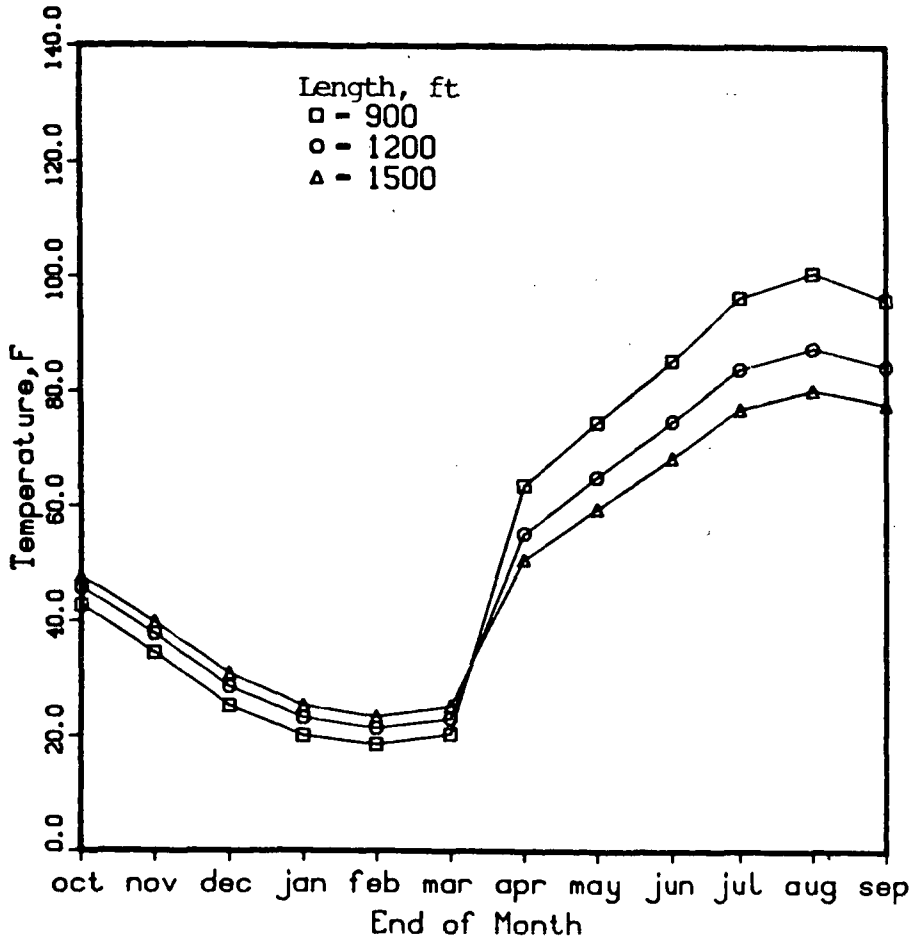

FIGURE 9. INLET FLUID TEMPERATURES TO HEAT PUMP WITH HORIZONTAL COIL IN PORTLAND, ME

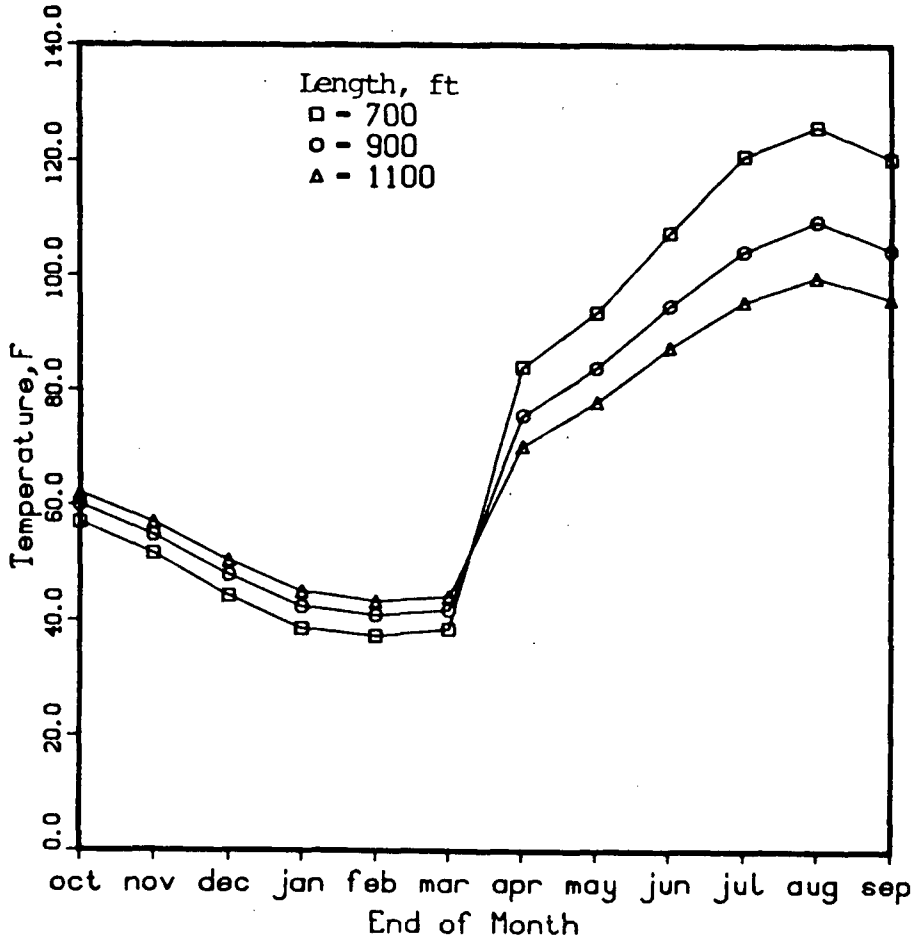

FIGURE 10. INLET FLUID TEMPERATURES TO HEAT PUMP WITH HORIZONTAL COIL IN ATLANTA, GA

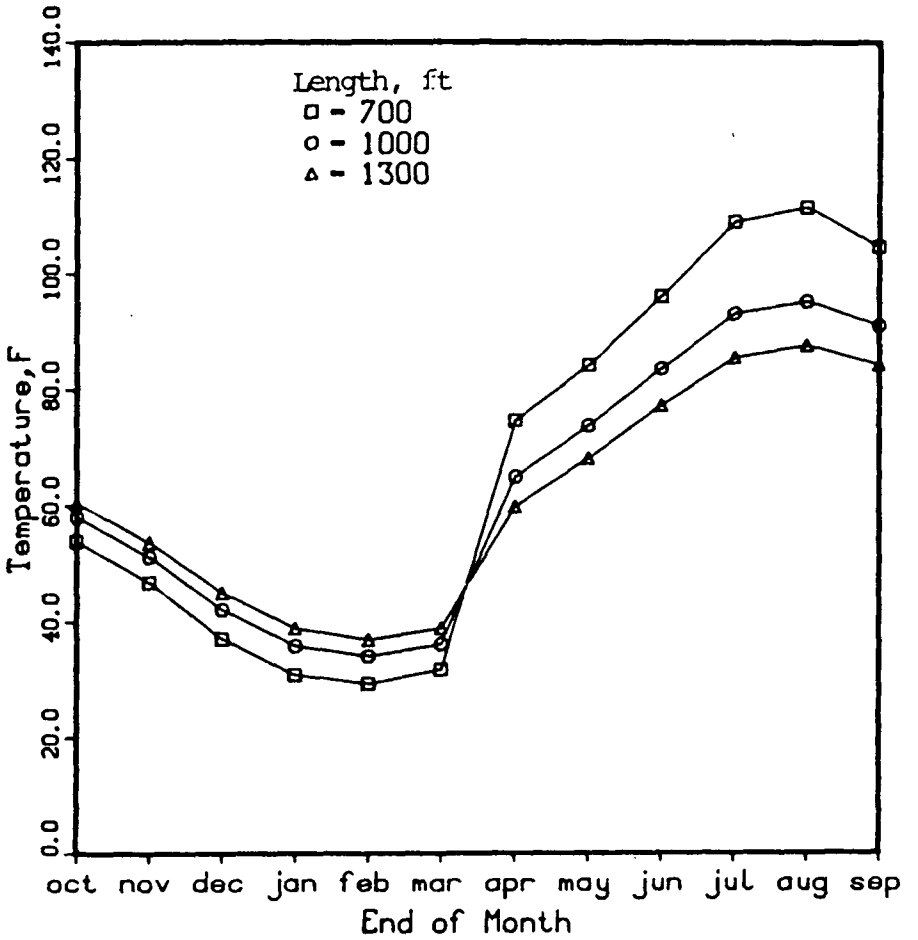

FIGURE 11. INLET FLUID TEMPERATURES TO HEAT PUMP WITH HORIZONTAL COIL IN WASHINGTON, D.C.

Data during the cooling season in Figure 10 for Atlanta, GA show a marked increase in inlet temperature when the coil length is marginally low. No freezing temperatures were evident in Atlanta even for the lowest coil length.

Plots such as Figures 10 and 11 can be used to assess the approach of coil length to the optimum based on performance considerations. For example, a coil length of about 900 ft appears to be about optimum, if freezing during heating and excessive temperatures during cooling are to be avoided.

Figures 12 to 14 show inlet fluid temperatures to the heat pump as a function of depth for a deep-well ground coil. The improved performance per unit length of the deep-well coil in comparison to that for the horizontal coil is attributable to more favorable earth temperatures and improved thermal properties of the rock layers which occur within 100 ft of the surface in all three cities.

Tables 16 to 18 show extremes of inlet fluid temperatures for all runs for the three coil types. Ideally, the different types of ground coils in each city, optimized based on performance, would have similar extremes of temperatures. For example, if one type of ground coil system had lower minimum temperatures than that for another type of coil in the same city, the coil with the lower temperature is undersized with respect to that for the other type. The same conclusion can be made with respect to the maximum temperatures; that is, a system with higher maximum temperatures is undersized. The data show that there were no gross discrepancies in sizing of one coil relative to another. This data will be helpful in selecting coil lengths or depths in any future refinement of this initial work.

Tables 19 to 21 show that values of seasonal coefficient of performance for heating with the ground-coil systems are substantially higher than that for air-source systems. For cooling operation, the seasonal coefficient of performance for ground coil systems is strongly affected by coil sizing. Values consistently lower than that for air-source systems were experienced in Phoenix and Houston. In other cities, values higher than that for air-source systems can be attained with properly sized coils.

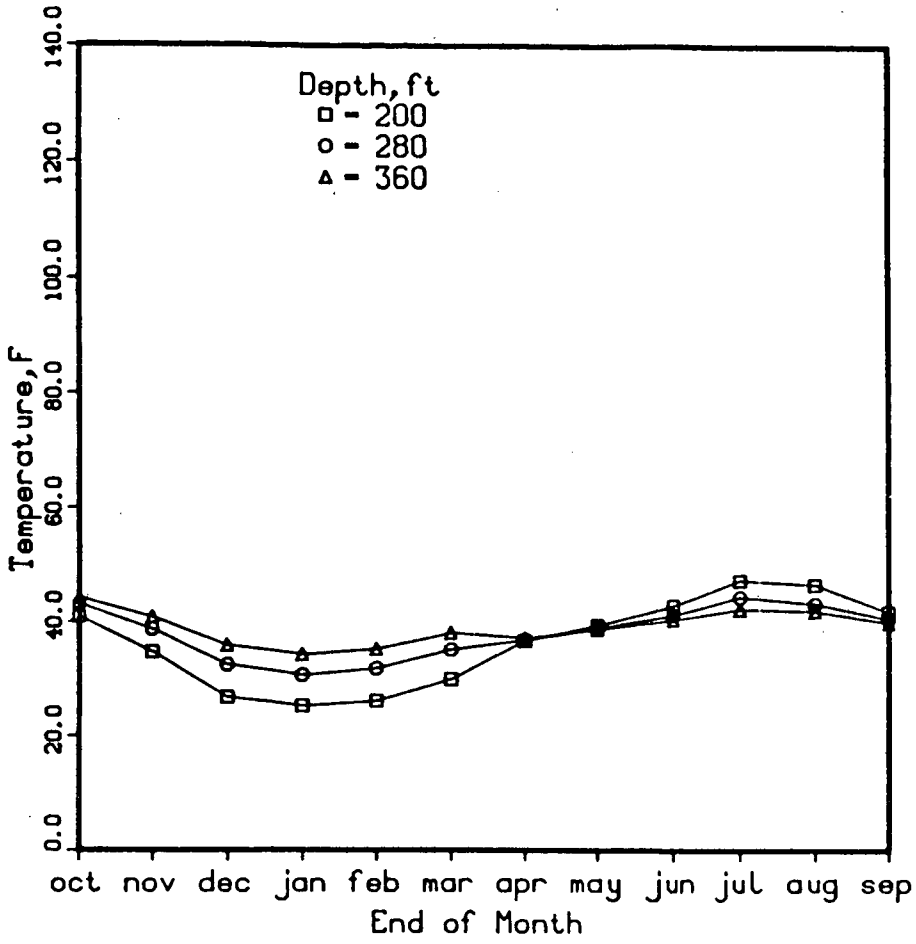

FIGURE 12. INLET FLUID TEMPERATURES TO HEAT PUMP WITH DEEP-WELL COIL IN PORTLAND, ME

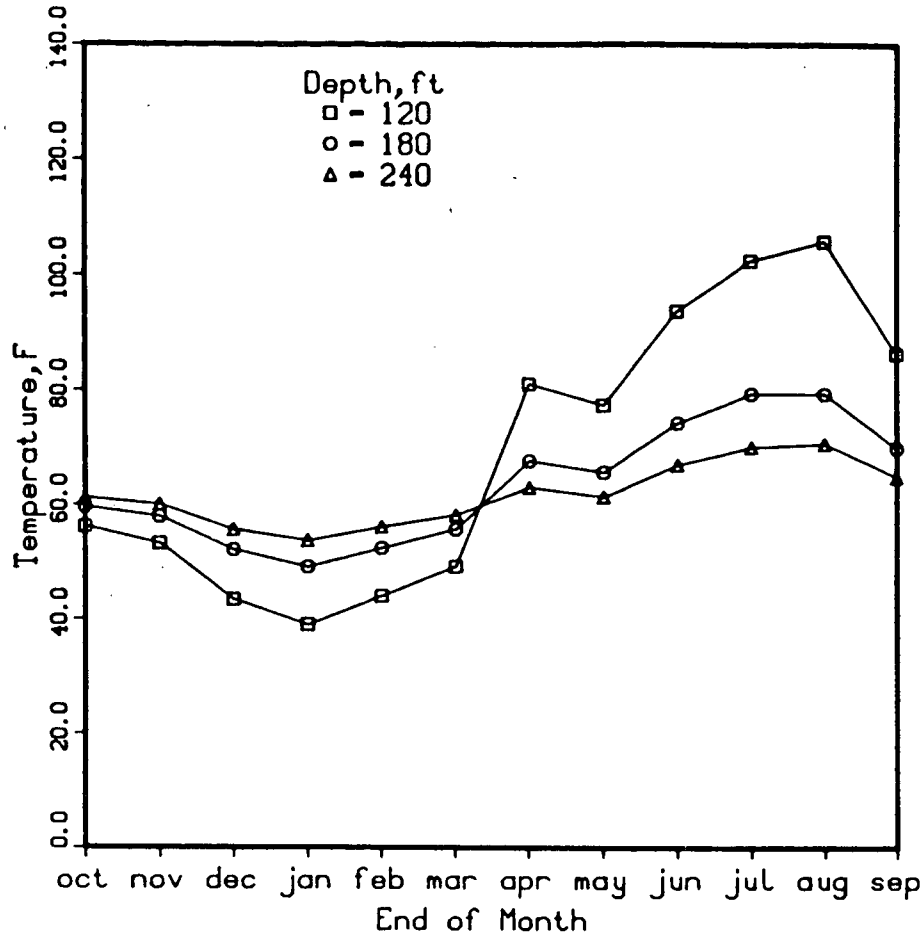

FIGURE 13. INLET FLUID TEMPERATURES TO HEAT PUMP WITH DEEP-WELL COIL IN ATLANTA, GA

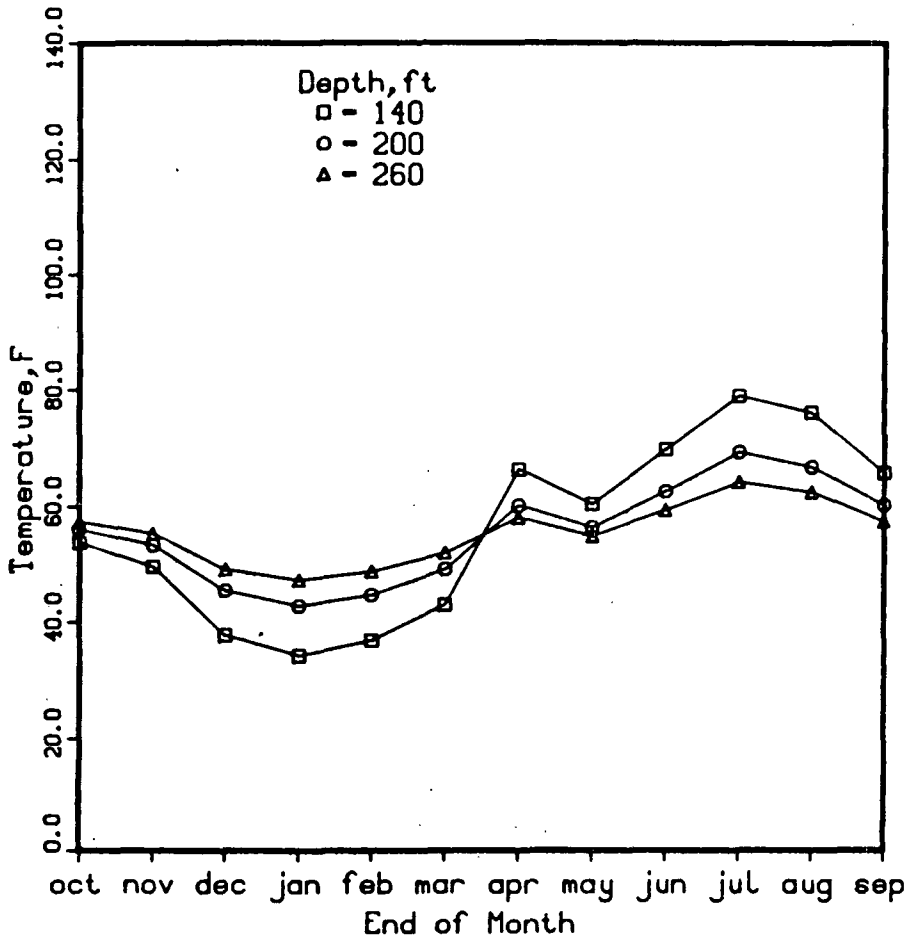

FIGURE 14. INLET FLUID TEMPERATURES TO HEAT PUMP WITH DEEP-WELL COIL IN WASHINGTON, D.C.

TABLE 16. INLET FLUID TEMPERATURES WITH HORIZONTAL GROUND COIL

City	Coil Length ft	End-of-Month Fluid Temperatures to Heat Pump, F Minimum	Maximum
Portland, ME	--	See Figure 9	
Atlanta, GA	--	See Figure 10	
Washington, D.C.	--	See Figure 11	
Pittsburgh, PA	1,200	28	89
Louisville, KY	900	30	113
	1,100	33	97
Phoenix, AZ	1,600	55	119
	1,800	55	108
Kansas City, MO	1,000	28	109
	1,100	29	98
Houston, TX	1,300	56	116
	1,500	58	104
Seattle, WA	500	26	122
	700	31	98
Minneapolis, MN	900	15	101
	1200	17	88

TABLE 17. INLET FLUID TEMPERATURES WITH DEEP-WELL GROUND COIL

City	Coil Depth, ft	End-of-Month Fluid Temperatures to Heat Pump, F Minimum	Maximum
Portland, ME	--	See Figure 12	
Atlanta, GA	--	See Figure 13	
Washington, D.C.	--	See Figure 14	
Pittsburgh, PA	240	36	56
	280	39	59
Louisville, KY	210	37	81
	250	41	73
Phoenix, AZ	400	66	125
	500	68	108
Kansas City, MO	210	36	73
	250	40	67
Houston, TX	340	68	108
	400	69	98
Seattle, WA	200	31	62
Minneapolis, MN	170	14	73
	250	23	60

TABLE 18. INLET FLUID TEMPERATURES WITH MULTIPLE, SHALLOW-WELL GROUND COIL

City	Coil		End-of-Month Fluid Temperatures to Heat Pump, F	
	No. of Tubes	Depth, ft	Minimum	Maximum
Portland, ME	9	80	29	44
Atlanta, GA	9	40	35	>130
	9	50	43	101
	9	60	47	87
Washington, D.C.	9	46	33	83
	9	60	41	72
Pittsburgh, PA	9	70	30	58
Louisville, KY	4	110	34	88
Phoenix, AZ	4	100	66	122
Kansas City, MO	4	100	36	73
Houston, TX	9	80	64	129
	9	100	66	122
Seattle, WA	4	70	30	67

TABLE 19. SEASONAL COEFFICIENT OF PERFORMANCE WITH HORIZONTAL GROUND COIL

City	Coil Length, ft	Heating COP		Cooling COP	
		Ground-Coil	Air-Source	Ground-Coil	Air-Source
Portland, ME	900	2.04	1.74	2.04	2.30
	1200	2.18		2.41	
	1500	2.25		2.60	
Atlanta, GA	700	2.83	1.89	1.57	2.35
	900	2.90		2.06	
	1100	2.94		2.36	
Washington, D.C.	700	2.61	1.84	1.83	2.32
	1000	2.74		2.33	
	1300	2.79		2.57	
Pittsburgh, PA	1200	2.57	1.79	2.54	2.28
Louisville, KY	900	2.62	1.83	1.81	2.33
	1100	2.70		2.17	
Phoenix, AZ	1600	2.96	1.97	1.52	2.15
	1800	2.95		1.66	
Kansas City, MO	1000	2.55	1.77	2.01	2.28
	1100	2.59		2.17	
Houston, TX	1300	3.04	1.97	1.67	2.31
	1500	3.04		1.89	
Seattle, WA	500	2.40	1.92	1.43	2.42
	700	2.60		2.11	
Minneapolis, MN	900	2.09	1.66	2.15	2.22
	1200	2.17		2.49	

TABLE 20. SEASONAL COEFFICIENT OF PERFORMANCE WITH DEEP-WELL GROUND COIL

City	Coil Length, ft	Heating COP		Cooling COP	
		Ground-Coil	Air-Source	Ground-Coil	Air-Source
Portland, ME	200	2.32	1.74	3.43	2.30
	280	2.56		3.55	
	360	2.66		3.61	
Atlanta, GA	120	2.87	1.89	2.00	2.35
	180	3.02		2.82	
	240	3.06		3.11	
Washington, D.C.	140	2.75	1.84	2.69	2.32
	200(1)	2.83		2.80	
	200	2.92		3.04	
	200(2)	2.96		3.16	
	260	2.98		3.20	
Pittsburgh, PA	240	2.77	1.79	3.43	2.28
	280	2.83		3.49	
Louisville, KY	210	2.80	1.83	2.67	2.33
	250	2.90		2.93	
Phoenix, AZ	400	3.09	1.97	1.51	2.15
	500	3.07		1.86	
Kansas City, MO	210	2.77	1.77	2.98	2.28
	250	2.85		3.15	
Houston, TX	340	3.11	1.97	1.89	2.31
	400	3.11		2.18	
Seattle, WA	200	2.61	1.92	3.38	2.42
Minneapolis, MN	170	1.88	1.66	2.81	2.22
	250	2.28		3.33	

(1) Inside dia of casing changed from 5.0" to 2.5"
(2) Inside dia of casing changed from 5.0" to 7.5"

TABLE 21. SEASONAL COEFFICIENT OF PERFORMANCE WITH MULTIPLE, SHALLOW-WELL GROUND COIL

City	Coil		Heating COP		Cooling COP	
	No. of Coils	Depth, ft	Ground-Coil	Air-Source	Ground-Coil	Air-Source
Portland, ME	9	80	2.39	1.74	3.49	2.30
Atlanta, GA	9	40	2.76	1.89	1.49	2.35
	9	50	2.91		2.22	
	9	60	2.97		2.65	
Washington, D.C.	9	46	2.71	1.84	2.60	2.32
	9	60	2.84		2.93	
Pittsburgh, PA	9	70	2.58	1.79	3.39	2.28
Louisville, KY	4	110	2.71	1.83	2.24	2.33
Phoenix, AZ	4	100	2.99	1.97	1.46	2.15
Kansas City, MO	4	100	2.74	1.77	2.85	2.28
Houston, TX	9	80	3.06	1.97	1.42	2.31
	9	100	3.05		1.52	
Seattle, WA	4	70	2.59	1.92	3.09	2.42

COST COMPARISONS

Feasibility assessment of ground coupling must consider costs as well as performance. We have shown that a substantial reduction in electrical power from that with air-source systems can be achieved with most of the ground-coupled systems run to date. This savings must be adequate to provide a payback of the additional costs attributable to the ground-coupled systems within a reasonable time to be of interest to the average homeowner. Some more affluent homeowners will be more interested in life-cycle cost savings.

Tables 22 to 24 show costs with horizontal, deep-well, and multiple, shallow-well systems compared to that for air-source systems. Heating and cooling costs are shown separately so that the positive or negative factors contributing to the annual power savings can be readily observed. Substantial annual power savings are evident for all systems for all cities except Phoenix, Houston, and Seattle. Annual power savings with each of the three systems configured for minimum simple payback were fairly equivalent.

Tables 22 to 24 also show simple payback of the additional costs attributable to the ground coil. Installed costs of the ground coil are based on costs listed in Table 5 with boring costs apportioned according to the soil layers as shown in Table 12. Costs for ground-coupled heat-pump components were not factored into the analysis because these costs should be about the same as for an air-source unit, since the cost for a brine pump and refrigerant-to-brine heat exchanger in a ground-coupled unit should be similar to that for the outdoor fan-coil unit and defrosting controls in an air-source unit.

Simple payback was lowest with horizontal and deep-well systems and was as low as 8.1 years in Portland, Maine. Simple payback was 10 years or less in four cities with deep-well systems and in two cities with horizontal systems. Simple payback with any system in cities with a high cooling load and deep water table as in Phoenix and Houston was excessive or nonexistent.

TABLE 22. COST COMPARISON WITH HORIZONTAL COIL

CITY	COIL LENGTH, FT	TOTAL ELECTRIC POWER COST, $ HEATING GROUND COIL	HEATING AIR SOURCE	COOLING GROUND COIL	COOLING AIR SOURCE	ANNUAL POWER SAVINGS, $	INSTALLED COST OF GROUND COIL, $	SIMPLE PAYBACK, YRS	LIFE-CYCLE COSTS AT 2.0 PERCENT DISCOUNT RATE, $ GROUND COIL	LIFE-CYCLE COSTS AT 2.0 PERCENT DISCOUNT RATE, $ AIR SOURCE	LIFE-CYCLE COSTS AT 10.0 PERCENT DISCOUNT RATE, $ GROUND COIL	LIFE-CYCLE COSTS AT 10.0 PERCENT DISCOUNT RATE, $ AIR SOURCE
PORTLAND, ME	900	739	867	116	103	119	1350	11.7	15326	15864	8624	8257
	1200	694		98		178	1800	10.1	14751		8541	
	1500	671		91		209	2250	10.8	14703		8732	
ATLANTA, GA	700	170	256	409	274	-49	1050	∞	10526	8661	5982	4508
	900	166		312		51	1350	26.3	9173		5422	
	1100	164		273		93	1650	17.7	8789		5366	
WASHINGTON DC	700	257	364	253	200	54	1050	19.4	9386	9219	5389	4798
	1000	245		198		121	1500	12.4	8743		5270	
	1300	240		180		144	1950	13.6	8818		5525	
PITTSBURGH, PA	1200	467	670	143	159	220	1800	8.2	11766	13566	6987	7061
LOUISVILLE, KY	900	203	291	277	216	27	1350	50.5	9200	8288	5436	4314
	1100	198		231		78	1650	21.2	8663		5300	
PHOENIX AZ	1600	86	130	781	556	-181	2400	∞	16584	11216	9783	5838
	1800	87		716		-116	2700	∞	15825		9532	
KANSAS CITY, KY	1000	273	393	309	273	84	1500	17.9	11023	10896	6457	5671
	1100	269		287		110	1650	15.0	10743		6383	
HOUSTON TX	1300	76	117	710	513	-154	1950	∞	14792	10308	8634	5365
	1500	76		626		-71	2250	∞	13726		8223	
SEATTLE, WA	500	116	145	30	18	17	750	44.4	3145	2672	1997	1391
	700	107		21		35	1050	29.6	3141		2138	
MINNEAPOLIS MN	900	714	781	143	139	63	1350	21.5	15368	15042	8646	7829
	1200	669		123		128	1800	14.1	14748		8539	

Note: Coil length not determined solely by economics. Limitations on ground coil fluid temperatures also a factor, as discussed on pp. 39 and 45. (Ref. Table 16 for pertinent fluid temperatures)

TABLE 23. COST COMPARISON WITH DEEP-WELL GROUND COIL

CITY	COIL DEPTH, FT	TOTAL ELECTRIC POWER COST, $ HEATING GROUND COIL	HEATING AIR SOURCE	COOLING GROUND COIL	COOLING AIR SOURCE	ANNUAL POWER SAVINGS, $	INSTALLED COST OF GROUND COIL, $	SIMPLE PAYBACK, YRS	LIFE-CYCLE COSTS AT 2.0 PERCENT DISCOUNT RATE, $ GROUND COIL	LIFE-CYCLE COSTS AT 2.0 PERCENT DISCOUNT RATE, $ AIR SOURCE	LIFE-CYCLE COSTS AT 10.0 PERCENT DISCOUNT RATE, $ GROUND COIL	LIFE-CYCLE COSTS AT 10.0 PERCENT DISCOUNT RATE, $ AIR SOURCE
PORTLAND, ME	200	651	867	69	103	250	2022	8.1	13792	15864	8148	8257
	280	591		67		312	2870	9.2	13626		8468	
	360	568		69		337	3719	11.0	14070		9107	
ATLANTA, GA	120	168	256	322	274	40	1148	29.1	9163	8661	5320	4508
	180	159		229		142	1785	12.6	8130		5087	
	240	157		207		165	2421	14.7	8382		5523	
WASHINGTON DC	140	244	364	172	200	148	1363	9.2	8168	9219	4905	4798
	200(1)	237		165		162	1742	10.8	8318		5165	
	200	230		152		182	2000	11.0	8247		5252	
	200(2)	227		146		191	2168	11.4	8269		5344	
	260	225		144		194	2636	13.6	8677		5780	
PITTSBURGH, PA	240	433	670	106	159	290	2426	8.4	11246	13566	7017	7061
	280	424		104		302	2851	9.4	11483		7344	
LOUISVILLE, KY	210	190	291	188	216	129	1968	15.3	8148	8288	5184	4314
	250	184		171		152	2393	15.8	8202		5417	
PHOENIX AZ	400	83	130	786	556	-182	3444	∞	17645	11216	10836	5838
	500	83		641		-38	4309	∞	16152		10471	
KANSAS CITY, KY	210	251	393	209	273	206	2016	9.8	9539	10896	5932	5671
	250	244		197		225	2441	10.8	9659		6198	
HOUSTON TX	340	74	117	625	513	-68	2927	∞	14356	10308	8876	5365
	400	74		544		13	3444	270.4	13544		8701	
SEATTLE, WA	200	107	145	13	18	44	1722	39.3	3677	2672	2740	1391
MINNEAPOLIS MN	170	847	781	109	139	-35	1464	∞	17089	15042	9596	7829
	250	636		92		192	2312	12.0	14211		8506	

(1) Inside diameter of casing changed from 5.0" to 2.5"
(2) Inside diameter of casing changed from 5.0" to 7.5"

Note: Coil depth not determined solely by economics. Limitations on ground coil fluid temperatures also a factor, as discussed on pp. 39 and 45. (Ref. Table 17 for pertinent fluid temperatures)

TABLE 24. COST COMPARISON WITH MULTIPLE SHALLOW-WELL GROUND COIL

CITY	COIL NO OF WELLS	COIL DEPTH, FT	TOTAL ELECTRIC POWER COST, $ HEATING GROUND COIL	HEATING AIR SOURCE	COOLING GROUND COIL	COOLING AIR SOURCE	ANNUAL POWER SAVINGS, $	INSTALLED COST OF GROUND COIL, $	SIMPLE PAYBACK, YRS.	LIFE-CYCLE COSTS AT 2.0 PERCENT DISCOUNT RATE, $ GROUND COIL	LIFE-CYCLE COSTS AT 2.0 PERCENT DISCOUNT RATE, $ AIR SOURCE	LIFE-CYCLE COSTS AT 10.0 PERCENT DISCOUNT RATE, $ GROUND COIL	LIFE-CYCLE COSTS AT 10.0 PERCENT DISCOUNT RATE, $ AIR SOURCE
PORTLAND, ME	9	80	634	867	68	103	269	4704	17.5	16170	15864	10672	8257
ATLANTA, GA	9	40	175	256	427	274	-71	1734	∞	11568	8661	6852	4508
	9	50	165		290		75	2387	32.0	9829		6261	
	9	60	162		243		125	3039	24.3	9659		6485	
WASHINGTON DC	9	46	248	364	178	200	138	2018	14.6	8976	9219	5639	4798
	9	60	236		158		170	2932	17.2	9371		6284	
PITTSBURGH, PA	9	70	465	670	107	159	258	3512	13.6	12863	13566	8379	7061
LOUISVILLE, KY	4	110	197	291	223	216	87	2241	25.9	9113	8288	5818	4314
PHOENIX AZ	4	100	86	130	816	556	-215	4569	∞	19304	11216	12238	5838
KANSAS CITY, KY	4	100	254	393	218	273	194	2031	10.5	9751	10896	6049	5671
HOUSTON TX	9	80	75	117	833	513	-277	3624	∞	18472	10308	11352	5365
	9	100	76		778		-223	4569	∞	18532		11836	
SEATTLE, WA	4	70	108	145	14	18	42	1401	33.6	3390	2672	2436	1391

Note: Coil length/depth not determined solely by economics. Limitations on ground coil fluid temperatures also a factor, as discussed on pp. 39 and 45. (Ref. Table 18 for pertinent fluid temperatures)

Deep-well systems clearly have lower simple payback than multiple shallow-well systems in Portland, ME and Washington, D.C. due to the improved properties of rock layers. Depth of multiple, shallow wells was selected for ease of drilling with a light rig, whereas a heavier-duty rig, used for drilling a deep well, could be used to bore into rock layers.

Life-cycle costs are shown in Tables 22 to 24 for discount rates of 2.0 percent and 10.0 percent. Life-cycle costs with a 2.0 percent discount rate for all three types of ground-coupled systems were lower than that for air-source systems in Portland, ME, Washington, D.C., Pittsburgh, Kansas City, and Minneapolis. In addition, similar values with deep-well ground-coupled systems were lower in Atlanta and Louisville. In our opinion, the slightly higher value shown for multiple, shallow-well systems in Portland, ME would have been lower with a larger coil.

Simple payback and life-cycle costs for systems in Seattle were adversely affected by low space conditioning loads and very low electrical power cost.

CONCLUSIONS AND RECOMMENDATIONS

Conclusions and recommendations based on results presented in Tables 13 to 24 are:

(1) Life-cycle costs with a 2.0 percent discount rate for all three types of ground-coupled systems were lower than that for air-source systems in five cities, and were lower in two additional cities with deep-well ground-coupled systems.

(2) Deep-well ground-coupled systems have lower simple payback than that for other types of ground-coil systems in seven cities, although payback for horizontal systems were about as good in two of these cities.

(3) Lowest simple payback for any system in any city was 8.1 years for deep-well systems in Portland, ME.

(4) Simple payback of 10 years or less appears to be feasible in four cities with deep-well systems and in two cities with horizontal systems.

(5) A deep-well ground-coupled system appears to be a strong competitor to a horizontal system in Portland, ME, Washington, D.C., and Pittsburgh. These results are probably influenced considerably by the good thermal properties assumed for rock layers, which were assumed to occur at depths of under 100 ft in these cities.

(6) Multiple shallow-well systems do not appear to be a clear choice over deep-well systems in any city. In cities with bed rock less than 100 ft. from the surface, such as Portland, ME, Washington, D.C., Atlanta, or Pittsburgh, the multiple shallow-well system was expected to be preferred due to lower drilling costs with the special-purpose Ditch-Witch machine, but the results didn't verify this expectation.

(7) Ground-coil systems do not appear to be appropriate for cities with a high cooling load, low heating load, low

water table, and no rock layers near the surface, such as Phoenix and Houston.

(8) In a city with low electrical rates, such as Seattle, recovery of additional costs due to the ground coil is difficult.

(9) Results from parametric study of the effect of casing diameter for deep-well systems show lowest life-cycle costs at 2.0 percent discount rate with the 5.0 inch casing but lowest simple payback with the 2.5 inch casing.

(10) Although the cost values assumed for this study are felt to be realistic, other cost scenarios for the ground coils should be explored using the performance data listed in Tables 13 to 15 for the three types of systems.

(11) Performance characteristics of the water-source heat pump were found to significantly affect the results. In our opinion, no current water-source unit is optimized for use in ground-coupling systems. For use in future parametric ground-coupling runs, performance characteristics of an "optimized" water-source heat pump should be prepared and compared to a similarly optimized air-source heat pump.

(12) Cycling losses for the ground-coupled heat pumps were only approximated in this initial study and probably were influenced by the size of heat pump selected for each city. An alternate approach to a constant degradation factor, used in this study, should be developed. One approach may be to use a single-node thermal-capacitance model for the building structure, a thermostat, and an exponential multiplier on capacity of the heat pump. Compressor power would be assumed to be constant but capacity would exponentially rise to the steady-state value for each inlet temperature.

(13) Future parametric runs should utilize a file of hourly ambient-temperature values extracted from representative hourly weather data for each city in order to provide more realistic random variations in this parameter. This change will affect both the building loads and performance of the air-source heat pump. In this study, monthly building loads from a bin analysis were matched using sinusoidally varying, typical day-of-the-month ambient temperature and appropriate building load parameters.

FUTURE WORK

Suggestions for future work are:

(1) Explore other cost scenarios for the ground coil using the available performance data (see Recommendation No. 11).

(2) Although realistic values have been chosen for variables felt to have a minor effect on the overall results, parametric study of values chosen for these variables should be conducted. Some of these variables include:

   (a) Coil material (polyethylene was assumed)

   (b) Coil wall thickness (0.125 inch was assumed)

   (c) Spacing of horizontal coils (4 ft. was assumed)

   (d) Spacing of multiple vertical coils to optimize interseasonal transfer of energy (8 ft. was assumed)

   (e) Width of soil in thermal contact with the coil (10 ft. radius assumed about the deep-well coil; 8 ft. width outer "store" in the multiple, shallow-well coil)

   (f) Thermal properties of various soil layers

   (g) Heat-pump cycling loss (0.15 assumed when capacity exceeded load during the timestep--this factor probably applied most of the time for heating because resistive heating was low.)

   (h) Cost of coil material, boring, or trenching and placement.

   (i) Long-term variation in temperature of the soil about the coil, particularly with multiple coils designed for interseasonal transfer of energy.

   (j) Temperature of the surface layer calculated from an energy balance rather than from the Kusuda relationship.

(3) No attempt was made to verify the accuracy of the Battelle-modified GROCS program used for performance analysis of

horizontal coils. This model should be verified using line-source theory. Alternately, it may be possible to work similar problems with horizontal and deep-well coil models by selecting appropriate input values and making minor modification to the source code.

(4) An attempt should be made to improve performance of ground-coupled systems in Houston and Phoenix.

(5) An attempt should be made to incorporate the effect of freezing of the soil about the coil into the models. This feature is particularly needed in the horizontal model. Frozen properties for top soil in each city are available from ORNL data. Estimates for heat of fusion would have to be made for each soil layer. Source codes would have to be modified to use "effective" properties for nodes in close proximity to the coil, which account for heat of fusion and frozen-volume fraction.

(6) Thermally-induced moisture transfer will be important for assessment of drying out of the coil during cooling operation with heat rejection to the ground, particularly in horizontal coils and in well-type coils placed above the water table. Since ground coupling appears to be favorable in mid-U.S.A. cities which have substantial cooling loads, some means for analysis of moisture movement in soils should be developed and applied to ground coupling. Several good codes are available but require further development to reduce computing time. Results in this study for cooling operation may be somewhat conservative, since wilting-dry soil properties were used for topsoil above the water table. However, performance of the ground coil would deteriorate rapidly, if a dry core formed around the coil.

REFERENCES

1. Ballou, M. L., et al, "MAD: A Computer Program for ACES Design Using Monthly Thermal Loads", ORNL Report No. ORNL/CON-51, March, 1981.

2. Eason, R. D. and Fenton, R. G., "A Comparison of Numerical Optimization Methods for Engineering Design", Trans. ASME, J. of Eng. for Industry, P. 196 (February, 1974).

3. Climatography of the United States No. 84, U.S. Weather Bureau.

4. "Typical Electrical Bills--January 1, 1982, U.S. Dept. of Energy, Energy Information Administration.

5. "Water-Source HVAC Design Manual, Seminar on Ground-Coil Heat-Pump Technology", conducted by Oklahoma State University, Oklahoma City (February, 1982).

6. Kusuda, T., et al, "Earth Temperatures and Thermal Diffusivity at Selected Stations in the United States", ASHRAE Trans., Vol. 71, Part 1, 1965.

7. Handbook of Tables for Applied Engineering Science, Second Edition, CRC Press, 1973.

8. Fischer, R. D. and Newman, D. C., "Design of Ground-Coupled Heat-Pump System for the UT Solar House", Battelle report to ORNL, November 19, 1981.

9. Parken, W. H., et al, "Factors Affecting the Performance of a Residential Air-to-Air Heat Pump", ASHRAE Trans. 81(1), pp 839-849 (1977).

10. Andrews, J. W., "A TRNSYS-Compatible Model of Ground-Coupled Storage", Brookhaven Labs Report No. BNL 51061, September, 1979.

11. Klein, S. A., et al, "TRNSYS--A Transient System Simulation Program", Eng. Exp. Sta. Report No. 38, University of Wisconsin, June, 1979.

12. Ball, D. A., et al, "State-of-the-Art Survey of Existing Knowledge of the Design of Ground-Source Heat Pumps", Battelle Report to ORNL, August 21, 1981.

13. Heaton, H. S., et al, "Heat Transfer in Annular Passages. Simultaneous Development of Velocity and Temperature Fields in Laminar Flow", Int. J. Heat and Mass Transfer, 17, pp 763-781, (1964).

14. Stickford, G. H., et al, "Numerical Simulation of Passive Solar Heating Systems", paper presented at San Diego Conference on Systems Simulation and Economic Analysis for Solar Heating and Cooling, 1978.

15. Ingersoll, L. R., et al, "Theory of Earth Heat Exchangers for the Heat Pump", Heating, Piping, and Air Conditioning, May, 1950.

16. Metz, P. D., "A Simple Computer Program to Model 3-Dimensional Underground Heat Flow with Realistic Boundary Conditions", ASME paper 81-WA/SOL-8, 10 pp, 1981.

INTERNAL DISTRIBUTION

1. V. D. Baxter
2. R. S. Carlsmith
3. F. A. Creswick
4. R. C. DeVault
5. J. E. Dobson
6. R. D. Ellison
7-10. P. D. Fairchild
11. S. K. Fischer
12. W. Fulkerson
13. V. O. Haynes
14. P. Intemann
15. F. R. Kalhammer, Consultant
16. S. V. Kaye, Consultant
17. T. R. LaPorte, Consultant
18. R. N. McGill
19. V. C. Mei
20. J. W. Michel
21. R. E. Minturn
22. W. R. Mixon
23. L. I. Moss, Consultant
24. J. C. Moyers
25. E. A. Nephew
26. W. H. Williams, Consultant
27-28. Central Research Library
29. Document Reference Section
30. Laboratory Records - RC
31-32. Laboratory Records Department
33. ORNL Patent Section

EXTERNAL DISTRIBUTION

34. Phil Albertson, Manager, Charles Machine Works, Inc., P.O. Box 66, Perry, OK 73077
35. C. H. Atkinson, Environmental Division, Acres Consulting Serv., Ltd., 5259 Dorchester Road, Niagara Falls, Ontario 12E G61
36. Falk Auer, Battelle Institute, e.V., Frankfurt, West Germany
37. B. Backstrom, Chalmers University of Technology, Jordvarme Gruppen, S-41296, Goteborg, Sweden
38. David A. Ball, Battelle Columbus Laboratories, 505 King Avenue, Columbus, OH 43201
39. Michael K. Bergman, Staff Scientist, American Public Power Assoc., 2301 M Street, N.W., Washington, DC 20037
40. W. Z. Black, Professor, School of Mech. Eng., GA Institute of Technology, Atlanta, GA 30332
41. Andrew L. Blackshaw, Manager, R&D, E-Tech, Inc., 3750 American Drive, Atlanta, GA 30341
42. James E. Bose, School of Technology, Oklahoma State University, Stillwater, OK 74078
43. David Cabot, President, Avondale Solar Corporation, P.O. Box 501, 44 Avondale Road, Westerly, RE 02891

44-74. James M. Calm, Project Manager, Heat Pump Development, Electric Power Res. Inst., 3412 Hillview Avenue, Palo Alto, CA 94303

75. Barry J. Dempsey, Dept. of Civil Engineering, University of Illinois, Urbana, IL 61801
76. R. J. Denny, Air-Conditioning & Refrigeration Institute, 1815 N. Fort Meyer Drive, Arlington, VA 22209
77. Richard Dougall, Dept. of Mechanical Engineering, University of

Pittsburgh, Pittsburgh, PA 15261

78. G. D. Duffy, Air Conditioning News, P.O. Box 2600, Troy, MI 48007
79. David G. Dutton, Vice President - Marketing, McElroy Manufacturing, Inc., P.O. Box 15580, Tulsa, OK 74112
80. John A. Edwards, North Carolina State University, Department of Mechanical and Aerospace Engineering, P.O. Box 5246, Raleigh, NC 27607
81. Don Ellis, Genesis Energy Systems, Div. of Hattersly & Sons, Inc., 3989 Mobil Avenue, Fort Wayne, IN 46896
82. Robert D. Fischer, Battelle Columbus Laboratories, 505 King Avenue, Columbus, OH 43201
83. R. J. Fiskum, Energy Conversion Equipment Branch, CE-113.2, Department of Energy, 1000 Independence Avenue S.W., Washington, DC 20585
84. Victor Goldschmidt, Ray W. Herrick Laboratories, Purdue University, W. Lafayette, IN 47907
85. E. Granryd, Dept. of Applied Thermodynamics and Refrigeration, Royal Institute of Technology, S-10044 Stockholm, Sweden
86. Robert M. Gregson, Vice President, Alten Northwest, 1134 Poplar Place, S., Seattle, WA 98144
87. G. C. Groff, Director, Research Division, Carrier Corporation, Carrier Parkway, Syracuse, NY 13201
88. Floyd Hayes, Thermal Systems, The Trane Company, 3600 Pammell Creek Road, LaCrosse, WI 54601
89. David Hodgett, Battelle Columbus Laboratories, 505 King Avenue, Columbus, OH 43201
90. Mark R. Hogan, Manager, Westinghouse Electric Corporation, R&D Center, Purdue Industrial Res. Park, 1291 Cumberland Avenue, West Lafayette, IN 47906
91. Michael Hughes, Friedrich Air Conditioning & Refrigeration, 2007 Beechgrove Pl., Utica, NY 13507
92. Patrick J. Hughes, P.E., W. S. Fleming & Associates, Inc., 5802 Court Street Road, Syracuse, NY 13206
93. G. Hultmark, Secretary, Chalmers Univ. of Technology, Jordvarme Gruppen, S-41296, Goteborg, Sweden
94. Douglas Jardine, Kaman Sciences Corporation, 1500 Garden of the Gods Rd., Colorado Springs, CO 80907
95. William S. Johnson, P.E., University of Tennessee, Energy, Environment and Resources Center, Knoxville, TN 37916
96. W. A. Jury, Assoc. Professor of Soil Physics, Dept. of Soil & Environ. Sci., University of California, Riverside, CA 92521
97. Mark Kalman, E-Tech Incorporated, 3570 American Drive, Atlanta, GA 30341
98. Herbert Kaufman, ARCO Comfort Products Company, 1271 Avenue of the Americas, New York, NY 10020
99. Richard Kurtz, Naval-Base-Housing Engineering, Naval Civil Engineering Lab., Port Hueneme, CA 93043
100. Edward A. Kush, 65 Crystal Rock Ct., Middle Island, NY 11953
101. Arvo Lannus, Residential & Commercial Applications, Electric Power Research Inst., 3412 Hillview Avenue, P.O. Box 10412, Palo Alto, CA 94303
102. Terry R. Larson, Marketing Services Manager, PLEXCO, 3240 N. Manniheim Road, Franklin Park, IL 60131

103. Calvin D. MacCracken, Calmac Manufacturing Company, 150 South Van Brunt Street, Englewood, NJ 07631
104. Philip Metz, Brookhaven National Laboratory, Building 701, Upton, NY 11973
105. P. Munter, Teknologisk Institut, Gregersensvej, DK-2630 Tastrup, Denmark
106. Joseph P. Murphy, Director of Education and Training, Oasis Energy Systems, 4425 N. High Street, Columbus, OH 43214
107. Richard A. O'Neil, Niagara Mohawk Power Corporation, 300 Erie Blvd. West, Syracuse, NY 13202
108. Sven G. Oskarsson, Cantherm, 8089 Trans-Canada Hwy., St. Laurent, Quebec H4S 1S4
109. Jerald Parker, School of Mechanical & Aerospace Eng., Oklahoma State University, 218 Engineer North, Stillwater, OK 74078
110. James R. Partin, GeoSystems, Inc., 3623 N. Park Drive, Stillwater, OK 74074
111. M. Porsvig, Danish Geotechnical Inst., 1 Maglebjergvej, DK-2800 Lyngby, Denmark
112. J. Rizzuto, New York State Energy Research & Development Auth., Agency Building No. 2, Rockefeller Plaza, Albany, NY 12223
113. G. Rosenbald, Chalmers University of Technology, Jordvarme Gruppen, S-41296, Goteborg, Sweden
114. J. D. Ryan, Energy Conversion Equipment Branch, CE-113.2, Department of Energy, 1000 Independence Avenue S.W., Washington, DC 20585
115. F. Schabkar, Graz University of Technology, Kopernikusgasse 24, A-8010 GRAZ, Austria
116. Ralph Schlichtig, P.E., Unconventional Heat and Power Sources, 11212 3rd Avenue, S., Seattle, WA 98168
117. A. H. Schroer, Sales Development Manager, Shell Chemical Company, Polybutylene Department, One Shell Plaza, P.O. Box 2463, Houston, TX 77002
118. Howard N. Shapiro, Dept. of Mech. Eng., Engineering Research Inst., Iowa State University, Ames, IA 50010
119. Graham Siegel, TVA Chattanooga, Research & Development, 1850 Commerce Union Bank Bldg., Chattanooga, TN 37401
120. Gary Skartvedt, American Heliothermal Corporation, Denver, CO 80222
121. Mason Somerville, Professor, Dept. of Mech. Eng., University of Arkansas, Fayetteville, AR 72701
122. Mario A. Sophocleous, Kansas Geological Survey, University of Kansas, Lawrence, KS 66044
123. Don Stephenson, National Research Council, Division of Buildings Res., Montreal Road, Ottawa, Canada KIA 0R6
124. Lee Sumner, Research Engineer, York Division, Borg-Warner Corporation, P.O. Box 1592, York, PA 17405
125. O. J. Svec, Geotechnical Section, Division of Building Research, National Research Council of, Canada, Ottawa, Ontario KIA 0R6
126. M. Keith Swinehart, Vanguard Plastics, Inc., 831 N. Vanguard Street, McPherson, KS 67460
127. Sherwood G. Talbert, Battelle Columbus Laboratories, 505 King Avenue, Columbus, OH 43201
128. Ralph Tilney, Alco Controls, 336 Chasselle, St. Louis, MO 63141

129. Jeffrey W. Wright, Engineering Consultant, Kansas Gas and Electric Co., Wichita, KS
130. Office of the Assistant Manager for Energy R&D, U.S. Department of Energy, Oak Ridge Operations, Oak Ridge, TN 37830
131-158. Technical Information Center, Department of Energy, P.O. Box 62, Oak Ridge, TN 37830